

**Cytochrome P450-3A4/Copper-Poly(propylene imine)-
Polypyrrole Star Co-polymer Nanobiosensor System for
Delavirdine – A Non-Nucleoside Reverse Transcriptase
Inhibitor HIV Drug**



By

Nomaphelo Ntshongontshi
W I (BSc Honours) P E

A mini-thesis submitted in partial fulfilment of the requirements for the degree
of

Magister Scientiae in Nanoscience

Faculty of Science

University of the Western Cape

Bellville, Cape Town, South Africa

Supervisor: Prof Emmanuel I. Iwuoha

November, 2014

Abstract

HIV and AIDS are among the world's pandemics that pose serious concern to almost every individual in the world. With the current level of availability of anti-retroviral (ARV) drugs and the ease of accessibility of treatment in many countries such as South Africa, the disease can be controlled by suppressing the viral load of an infected individual. These anti HIV drugs such as delavirdine are metabolised by enzymes which are found in the liver microsomes, particularly those of the cytochrome P450 family. Due to the fact that the metabolic rate of a patient determines the effect of the drug, the drug could either have a beneficial or an adverse effect once it is administered. It is therefore imperative that the metabolic profile of a patient is determined at point-of-care is necessary for proper dosing of the ARV drugs. In this project a nanobiosensor system was devised and used for the determination of the metabolism of delavirdine, a non nucleoside reverse transcriptase inhibitor (NNRTI) ARV drug. The nanobiosensor was prepared by the entrapment of the isoenzyme CYP3A4 into a pre-formed electro active carrier matrix consisting of a dendrimeric copper generation-2 poly(propylene imine)-co-polypyrrole star copolymer (Cu(G2PPI)-co-PPy). The metallo-dendrimer was used as a host for the enzyme and provided the necessary bio-compatible environment that allowed the direct transfer of electrons between the enzyme's active centres and platinum electrode surface. Copper was the choice of metal used in the study due to its properties. Copper is a malleable, ductile and a good conductor of both heat and electricity. It is a better conductor than most metals. Silver which also belongs to group 1b in the periodic table is a better electrical conductor than copper but copper has better corrosion resistance and is a more abundant and hence it is a cheaper material to use. Cu(G2PPI)-co-PPy was prepared by the incorporation of the copper metal into the G2PPI and the electropolymerization of pyrrole onto the Cu(G2PPI). The incorporation of Cu into G2PPI was determined by FTIR which did not show the presence of the Cu but showed an increase in the intensities of the peaks after the incorporation. The surface morphology of Cu(G2PPI) was confirmed by the use of HRSEM which showed a difference in the surface morphology of the dendrimer moiety with the addition of the copper metal. The HRSEM images after Cu incorporation resulted in the change from rough surface to smooth surface with open cavities which were essential for the entrapment of the biological systems (CYP3A4). Energy dispersive spectrometry (EDS) and HRTEM were used to confirm the presence of spherically shaped copper nanoparticles in the Cu(G2PPI) and were found to have a size distribution of 12-17 nm with an average particle size of 15

nm. The star copolymer (Cu(G2PPI)-co-PPy) was characterised using cyclic voltammetry where it was confirmed that the material was electroactive and conducting due to electron movement along the polymer chain. A diffusion co-efficient (D_o) value of $8.64 \times 10^{-5} \text{ cm}^2/\text{s}$ was determined for the material indicating a slow electron transfer kinetics within the diffusion layer. The constructed nanobiosensor was developed using copper poly(propylene imine) – polypyrrole star copolymer, bovine serum albumin and glutaraldehyde coupled to the enzyme CYP3A4. The resultant nanobiosensor parameters include a dynamic linear range (DLR) of 0.01-0.06 nM, a limit of detection (LOD) of 0.025 nM and a sensitivity value of $0.379 \mu\text{A}/\text{nM}$.



Key words

Biosensor

Dendrimers

Metallo-dendrimers

Cytochrome P450 (CYP3A4)

Delavirdine drug

Limit of detection (LOD)

Dynamic linear range (DLR)

Metabolism

Cyclic voltammetry (CV)

Star copolymer

Non Nucleoside Reverse Transcriptase Inhibitors (NNTIs)



Declaration

I declare that “*Cytochrome P450-3A4/copper-poly(propylene imine)-polypyrrole star copolymer nanobiosensor system for delavirdine – a non-nucleoside reverse transcriptase inhibitor HIV drug*” is my own work, that it has not been submitted before for any degree or examination in any other university, and that all the sources I have used or quoted have been indicated or acknowledged as complete references.



Nomaphelo Ntshongontshi

November 2014

Signed

Acknowledgement

To the Lord almighty thank you for granting me strength and the courage to complete my work through the difficult times.

To my supervisor, Prof Emmanuel Iwuoha a big and special thanks for the encouraging words when I had no hope, for the support that you gave me and ensuring me that I can do better than what I thought I could. Also thank you for the supervision and guidance that you have given me throughout my work.

To Dr Fanelwa Ajayi and Dr Abdul Baleg your support and encouragement has gone a long way. I am thankful for working under your supervision.

To the staff of the Chemistry department and Sensorlab members, thank you for the patience, the love and the support you have given me. Your help is highly appreciated.

To my family and friends without your love, patience, encouragement and support I wouldn't be where I am today. You are sincerely appreciated. Thank you.

Thank you to the Department of Science and Technology for the opportunity and the funding you gave me throughout the completion of the study.



Dedication

This thesis is dedicated to my late brother Lusindiso Ntshongontshi. To my parents Nothembisile and Qinisile Ntshongontshi, my siblings Lwandile Ntshongontshi, Akhona Ntshongontshi, Tembisa Ntshongontshi, Veliswa Ntshongontshi and Aphelele Ntshongontshi



Table of contents

Abstract	ii
Key words	iv
Declaration	v
Acknowledgement	vi
Dedication	vii
List of abbreviations	x
List of figures	xiii
List of tables	xv
Chapter 1	xvi
Introduction	xvi
Background	1
1.2 Problem statement.....	5
1.3 Rational and motivation	5
1.4 Aim and objectives	6
1.5 Thesis lay-out	8
Chapter 2	9
Literature review	9
2.1 Drug metabolism.....	10
2.2 Delavirdine drug	12
2.3 Dendrimers.....	13
2.3.1 Types of dendrimers	14
2.3.1.1 Poly (Propylene imine) dendrimers	14
2.3.1.2 Metallodendrimers	15
2.4 Polymers	16
2.4.1 Conducting polymers	16
2.4.1.1 Polypyrrole	17
2.4.1.2 Electrochemical polymerization of pyrrole.....	18
2.4.1.3 Star copolymers.....	18
2.5 Biosensors	19
2.5.1 Electrochemical biosensors.....	20
2.5.1.1 Amperometric biosensors	21

2.5.1.2 Potentiometric biosensors	21
2.5.1.3 Impedimetric biosensors	22
2.6 Enzyme	23
2.6.1 Cytochrome P450.....	23
2.6.2 Mechanism of CYP450 Enzyme complex.....	25
Chapter 3	26
Experimental methods.....	26
3.1 Reagents.....	27
3.2 Instrumentation	27
3.2.1 Spectroscopic techniques	28
3.2.1.1 Fourier transform infra-red spectroscopy (FTIR)	28
3.2.1.2 Energy dispersive spectroscopy (EDS).....	28
3.2.2 Microscopic techniques.....	29
3.2.2.1 High resolution transmission electron microscopy (HRTEM)	29
3.2.2.2 High resolution scanning electron microscopy (HRSEM).....	29
3.2.3 Electrochemical techniques.....	30
3.2.3.1 Cyclic Voltammetry (CV).....	30
3.3 Methodology	31
3.3.1 Synthesis of 2-Pyrrole functionalized Poly(propylene imine) dendrimer (PPI-2Py).....	31
3.3.2 Synthesis of generation 2 copper metallodendrimer	31
3.4 Pre-treatment of working electrode.....	31
3.4.1 Electrochemical polymerization of pyrrole on Pt electrode.....	31
3.4.2 Electrochemical polymerization of Pyrrole on Pt electrode surface coated with G2Cu-PPI-2Py	32
3.4.3 Fabrication of biosensors	32
3.4.3.1 Fabrication of CYP3A4 biosensor: CYP/Pt.....	34
3.4.3.2 Fabrication of CYP 3A4 biosensor: (Cu(G2PPI)-co-PPy)/BSA/Glu/Pt	34
3.5 Preparation of Delavirdine stock.....	34
Chapter 4	35
Results and discussion	35
4.1 Spectroscopic characterisation of G2 PPI-2Py and (Cu(G2PPI-2Py)	36
4.1.1 Fourier transformed infrared spectroscopy (FTIR).....	37
4.2 Microscopic characterisation of G2PPI-2Py and (Cu(G2PPI-2Py)	39
4.2.1 High resolution scanning electron microscopy (HRSEM).....	39

4.2.2 High resolution transmission Electron Microscope (HRTEM).....	41
4.2.3 Energy dispersive spectroscopy (EDS).....	43
4.3 Electrochemical polymerization characterisation of PPy and (Cu(G2PPI)-co-PPy)	44
Chapter 5	53
Characterization of CYP 3A4 nanobiosensor and detection of DLV	53
Chapter 6	63
Conclusion and recommendations	63
Chapter 7	66
References.....	66



List of abbreviations

Abbreviations	Definitions
HIV	Human immunodeficiency virus
PPI	poly(propylene imine)
PPy	Polypyrrole
Cu	Copper
AIDS	Acquired immunodeficiency syndrome
HAART	Highly active antiretroviral therapy
ART	Antiretroviral therapy
WHO	World Health Organization
CYP3A4	Cytochrome P450-3A4 enzyme
PBS	Phosphate buffer solution
PtE	Platinum electrode
FT-IR Fourier	Fourier Transformation Infrared spectroscopy
CV	Cyclic voltammetry
EDS	Energy dispersive spectrometry (spectroscopy)
HRSEM	High resolution scanning electron microscopy
HRTEM	High resolution transmission electron microscopy
G2	Generation 2
(Cu(G2PPI)-co-PPy)	Copper generation-2 poly(propylene imine)-co-polypyrrole star copolymer

(Cu(G2PPI))	Copper generation-2 poly(propylene imine)
(Cu(G2PPI-2Py))	Copper generation-2 poly(propylene imine)-2 Pyrrole
G2PPI	Generation 2 poly(propylene imine)
G2PPI-2Py	Generation 2 poly(propylene imine)-2Pyrrole
POPAM	Poly (Propylene Amine)
DLR	Dynamic linear range
LOD	Limit of detection
D _o	Diffusion co-efficient
NNRTIs	Nucleoside Reverse Transcriptase Inhibitors
DLV	Delavirdine
E _{pc}	Cathodic peak potential
E _{pa}	Anodic peak potential
C _{max}	Highest observed plasma concentration
E ⁰	Formal potential

List of figures

Figure 1: Key aspects of the HIV life cycle.

Figure 2: Structure of delavirdine.

Figure 3: Hyperbranched/ tree-like structure of dendrimers.

Figure 4: Structure of PPI dendrimer.

Figure 5: Structure of polypyrrole.

Figure 6: Biosensor components.

Figure 7: Catalytic cycle of CYP.

Figure 8: Schematic representation for development of CYP3A4/(Cu(G2PPI)-co-PPy)/Pt.

Figure 9: FTIR spectra of (Cu(G2PPI-2Py) and G2PPI-2Py.

Figure 10: The High Resolution Scanning Electron Microscopy (HRSEM) images of G2PPI-2Py (A) and (Cu(G2PPI-2Py) (B).

Figure 11: The High Resolution Transmission Electron Microscopy (HRTEM) images of G2PPI-2Py (A) and (Cu(G2PPI-2Py) (B).

Figure 12: The Energy Dispersive X-ray radiation (EDX) Spectrum of the (Cu(G2PPI-2Py) (A) and (B) G2PPI-2Py.

Figure 13: Electrochemical polymerization of Py onto Pt electrode in 0.1 M lithium perchlorate (+800 mV) to (-800 mV) at scan rate 50 mV/s.

Figure 14: Cyclic voltammogram of PPy/Pt electrode in 0.1 M pH 7.4 phosphate buffer at scan rates (10 mV/s to 100 mV/s).

Figure 15: Randle Sevcik plot of PPy in 0.1M phosphate buffer PH 7.4 at different scan rates for the determination of the diffusion co-efficient.

Figure 16: Electropolymerization of Py onto Cu-PPI-2py/Pt electrode in 0.1 M lithium perchlorate at 50mV/s.

Figure 17: Cyclic voltammogram of (Cu(G2PPI)-co-PPy)/Pt in 0.1 M PBS pH 7.4 at the potential window of +800 mV to -800 mV.

Figure 18: Randle Sevčik plots of (Cu(G2PPI)-co-PPy)/Pt at different scan rates studied in 0.1 M PBS, pH 7.4 for determination of the diffusion co-efficient D_0 .

Figure 19: Cyclic voltammogram of PPy//Pt, Cu(G2PPI) and Cu(G2PPI)-co-PPy//Pt in 0.1M PBS pH 7.4 buffer at 50 mV/s.

Figure 20: Reaction scheme showing the metabolism of delavirdine using the CYP 3A4/(Cu(G2PPI)-co-PPy) /Pt nanobiosensor.

Figure 20(A) and (B): Structures of delavirdine and indole carboxylic acid respectively.

Figure 21: Cyclic voltammograms of the nanobiosensor at different scan rates (10, 20, 30, 40, 50, 60, 70, 80 and 90 mV/s) in 0.1 M PBS pH 7.4.

Figure 22: Randle Sevčik plot of CYP 3A4/(Cu(G2PPI)-co-PPy)/Pt biosensor in 0.1M PBS pH 7.4 at different scan rates for the determination of the diffusion co-efficient.

Figure 23: Cyclic voltammograms of the Pt electrode, CYP3A4/PtE and CYP3A4/(Cu(G2PPI)-co-PPy)/PtE nanobiosensor in PBS pH 7.4.

Figure 24: Cyclic voltammograms of the CYP 3A4/(Cu(G2PPI)-co-PPy)/Pt under aerobic and anaerobic conditions in 0.1M PBS PH 7.4 at scan rate 10 mV/s.

Figure 25: Cyclic voltammogram of the CYP3A4/(Cu(G2PPI)-co-PPy)/Pt nanobiosensor response of DLV drug in 0.1M PBS pH 7.4.

Figure 26: Calibration curve from the linear range of hyperbolic curve for the determination of the LOD.


List of tables

Table 1: Bonds and their respective frequencies in the structure of the G2PPI-2Py and (Cu(G2PPI-2Py) metallodendrimer.

Table 2: Electrochemical studies of PPy and (Cu(G2PPI)-co-PPy).

Table 3: Detection limits for delavirdine by different detection methods.





Chapter 1
Introduction
WESTERN CAPE

1.0 Summary

This chapter gives a brief overview on the background of the human immunodeficiency virus (HIV) and its life cycle, the process of anti-retroviral treatment (ART) and a description of anti retroviral drugs. This chapter also includes the problem statement, motivation, aim and objectives and the outline of this document.

Background

Human immunodeficiency virus (HIV) is a retrovirus that leads to the formation of acquired immunodeficiency syndrome commonly known as AIDS. HIV attacks the cells of the body that are required for protection against foreign substances such as diseases. During HIV infection, the virus attacks and destroys the infection-fighting CD4 cells of the body's immune system. CD4 cells are T helper lymphocytes which are white blood cells that help the immune system to coordinate the attack of foreign organisms (Cornell, 1997). Although the HIV virus is able to infect a variety of cell types, acquired immunodeficiency syndrome (AIDS) results from the depletion of CD4+ T-Helper lymphocyte cells, a key component of the human immune system. The envelope (env) gene encodes the proteins of the outer envelope of the virus, the group-specific antigen (gag) gene encode the components of the inner capsid protein, whereas the polymerase (pol) gene codes for the enzymes such as Reverse transcriptase that are used in viral replication. Even though it mostly attacks these cells it also affects other cells of the body in order to stay in a dominant phase. HIV makes copies of itself and infects other cells by using the CD4 cells as the host cells. This process causes a reduction of CD4 cell thus weakening the immune system against infections. The time taken for the HIV virus to progress to AIDS varies with each person. Therefore, may take a couple of years before HIV develops to AIDS (Crumbliss, 1992).

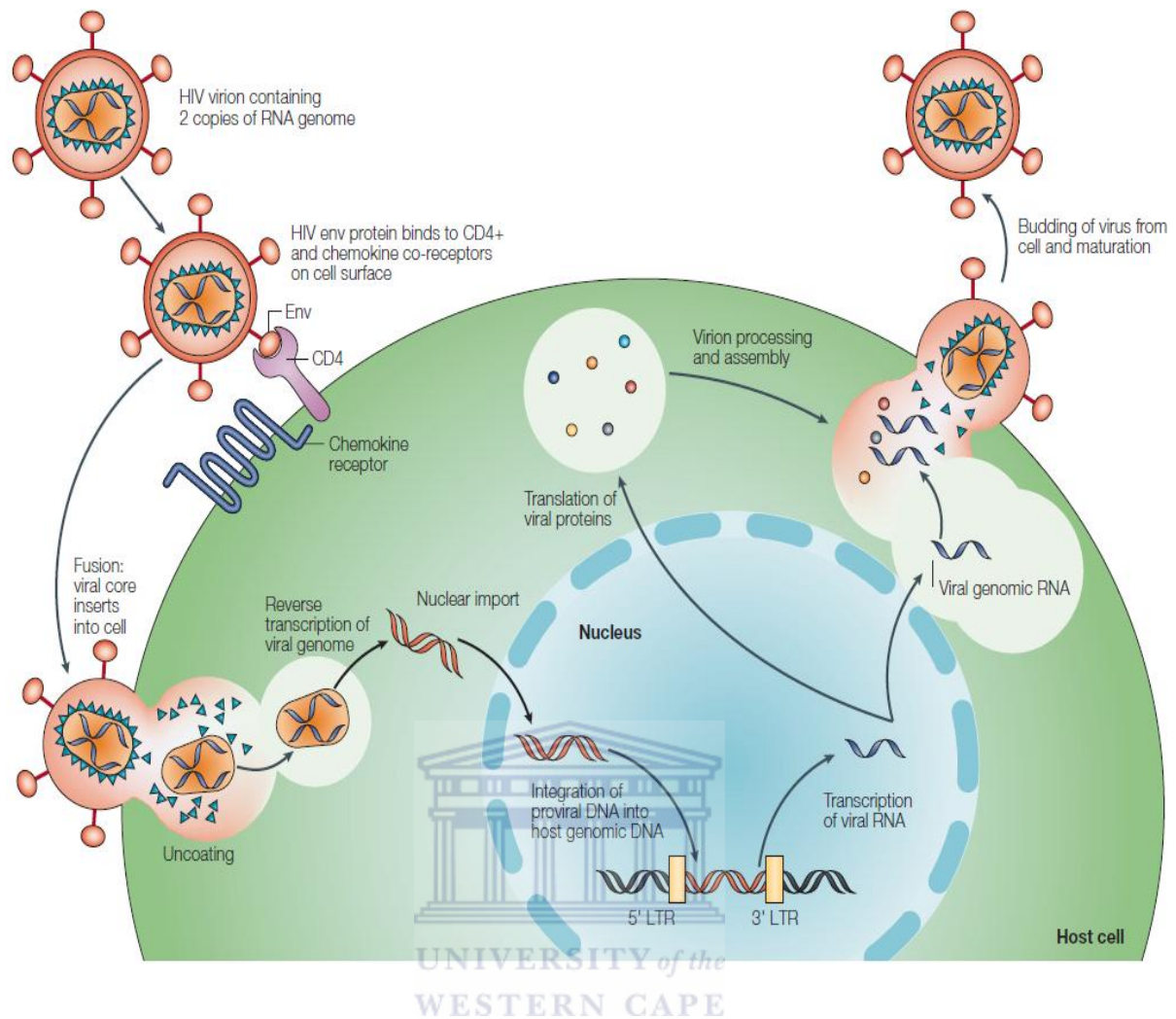


Figure 1: Key aspects of the HIV life cycle (Kirchheiner, 2007).

The virus can be transmitted from one person to another through infected blood, semen or vaginal secretion in contact with an infected person's broken skin or mucous membranes (a mucous membrane is wet, thin tissue found in certain openings to the human body). In addition, pregnant women who are infected can transmit the virus to their baby during pregnancy or during the course of delivery and/or during breast feeding. Once the virus is transmitted through any of the above mentioned measures it enters the body and binds to the CD4+ cell through its protein envelope on the surface of the host cell. The HIV envelope and the CD4 cell membrane fuse together allowing the penetration of the virus into the CD4 cell. Once inside the cell, HIV releases an HIV enzyme called reverse transcriptase which it used for the conversion of its genetic material from HIV RNA to HIV DNA. This conversion is necessary so that HIV can enter the nucleus of the CD4 cell and combine with its genetic

material. HIV produces an enzyme called integrase whose function is to allow the HIV DNA to enter the CD4 cell nucleus; once inside it integrates with the CD4 cell DNA. Once HIV is integrated into the DNA of the cell it uses the machinery of the CD4 cell to make long chains of the HIV protein which are the building blocks for HIV duplication. The long chains are cut into smaller chains by an enzyme known as protease, the combination of the smaller proteins forms a new virus, and the newly formed HIV virus exits within the cell, this process is known as the HIV life cycle and is described in Fig.1 (Kirchheiner, 2007).

HIV is a world pandemic where the number of people affected by the disease is constantly increasing each year. At the end of 2013, there were 35 million [33.2 million–37.2 million] people living with HIV. This number is increasing as more people are living longer because of antiretroviral therapy, alongside the number of new HIV infections-which, although declining, is still very high. An estimated 0.8% [0.7–0.8%] of adults aged 15–49 years worldwide are living with HIV, although the burden of the epidemic continues to vary considerably between regions and countries. There are 3.2 million [2.9 million–3.5 million] children younger than 15 years living with HIV and 4 million [3.6 million–4.6 million] young people 15–24 years old living with HIV, 29% of whom are adolescents aged 15–19 years. There are 16 million [15.2 million–16.9 million] women aged 15 years and older living with HIV; 80% live in sub-Saharan Africa. The primary contributor to the scale of the epidemic in this region is heterosexual transmission and the increased vulnerability to and risk of HIV infection among adolescent girls and young women.

Of the 35 million people living with HIV, 24.7 million [23.5 million–26.1 million] are living in sub-Saharan Africa, the region hardest hit by the epidemic. Nearly one in every 20 adults is living with the virus in this region. Almost 4.8 million [4.1 million–5.5 million] people are living with HIV in Asia and the Pacific, although the regional prevalence of HIV infection is about one-seventeenth than in sub-Saharan Africa. In the Caribbean, 1.1% [0.9–1.2%] of adults were living with HIV at the end of 2013 (Rambaut, 2004).

The most common problem with HIV is the fact that it has no cure. However there are drugs available that help with the drastic change in the progression time between the infection of HIV and its development into AIDS. The development of safe and effective drugs ensures that HIV positive people live a longer and healthy lives further increases their life expectancy (Belluzo, 2008).

The current drugs available do not cure HIV infections but they do however prevent the development of AIDS. The drugs do not eliminate the virus from the body but prevent the virus from being made in the body, stopping the virus from weakening and damaging the immune system (Xiao, 2013). As HIV attacks the CD4 cells, they deplete in number. This depletion in CD4 cells signifies the weakening of the immune system showing inability to fight opportunistic diseases and infections such as Tuberculosis (TB) and pneumonia. This means the immune system needs help so it can regain its strength and ability to fight off any infections or diseases. There are factors that determine the time a patient needs to start going into the anti-retroviral treatment. These factors include the CD4 count which determines the number of CD4 cells that are present in the blood which determines how well the immune system is working and the determination of the viral load which measures the amount of the HIV virus in the blood. Having a low CD4 count and a high viral load means that a patient needs to start taking the anti-retroviral drugs so they can increase the CD4 cell count and decrease the viral load (Bistolos, 2005).

Anti-Retroviral Treatment (ART) is the recommended HIV treatment. It is a combination of different drugs that needs to be taken every day at the same time. The combination ARV therapy prevents the HIV virus from multiplying inside a persons body. When the virus stops making copies of itself then the body's immune cells most notably the CD4 cells are able to live longer and provide the body protection from infections. HIV is an active virus and constantly makes copies of itself damaging the body's immune cells. It can adapt very quickly to medicine by changing itself through gene mutation (Chemla, 2000). Taking a combination of different drugs at the same time in the same way ever day decreases the chances of the virus multiplying thus making the resistance of the virus to the drugs hard. Missing the medication increases the risks of resistance of the virus to the ART. The multiplication of the virus takes place inside an infected cell where the virus makes copies of itself and can infect other cells of the body. Anti-retroviral drugs interfere with the multiplication process and how it spreads to other cells (Boozer, 2003).

There are different classes of HIV drugs. These include Nucleoside Reverse Transcriptase Inhibitors (NNRTIs): these drugs bind to and alter reverse transcriptase, an enzyme HIV needs to make copies of itself. Non-Nucleoside Reverse Transcriptase Inhibitors (NNRTIs): NRTIs block reverse transcriptase, an enzyme HIV needs to make copies of itself. Protease

Inhibitors (PIs): PIs block HIV protease, an enzyme HIV needs to make copies of itself. Fusion Inhibitors: Fusion inhibitors block HIV from entering the CD4 cells of the immune system. CCR5 Antagonists: CCR5 entry inhibitors block CCR5, a protein on the CD4 cells that HIV needs to enter the cells. Integrase Inhibitors: Integrase inhibitors blocks HIV integrase, an enzyme HIV needs to make copies of itself and Fixed-Dose Combination: Fixed-dose combination tablets contain two or more anti-HIV medications from one or more drug classes (Voorman, 1999).

1.2 Problem statement

HIV is a world pandemic which affects every individual (Rambaut, 2004). The availability of treatment to HIV infected patients has decreased the mortality rate caused by AIDS. The treatment manages to decrease the viral load and boosts the immune system. It fails to meet the individual required doses of patients. Even though there is availability of treatment which has decreased the mortality rate of HIV infected patients different individuals have different drug metabolic rates, this leads to the drug being ineffective to some individuals. The most viable solution to this problem is the identification of poor, intermediate and rapid metabolizers through finding a rapid device that detects and quantifies the amount of drug in the human system after administration.

1.3 Rational and motivation

Sometimes there are different and undesired effects of certain drugs in different populations. This is particularly true for the drug having narrow therapeutic index. Often these different effects are detrimental to an individual, thus termed as adverse drug reactions. Many patients die from these adverse drug reactions and due to failure of the immune system they struggle to respond to the drug or poor administration of the drug. The other problem is that there is the fact that different individuals have different metabolic rates to drugs. There are three known types of metabolizers, rapid metabolizers, intermediate metabolizers and poor metabolizers. Metabolic rates depend mainly on cytochrome P-450 and N-acetyltransferase enzymes. Patients may be classified as fast, intermediate or slow metabolizers, depending on the activity levels of these enzymes. Poor metabolizers: have slow metabolic rates which

result in high drug plasma concentration. In case of fast/ ultrarapid metabolizers they have fast metabolic rates. Due to their fast metabolic rates the therapeutic effect may be diminished or absent (Varshney, 2012).

It is common in medicinal and clinical practises to administer the same amount/ dose of drugs to all patients, leading to differences in the plasma concentrations of the drugs which correlates with the patients genotype. High drug concentration has detrimental effects on the patients as it causes concentration related central nervous system toxicity. Devising a nanobiosensor system which can be used for the monitoring of the metabolism of a drug such as delavirdine; a non nucleoside reverse transcriptase inhibitor will aid in determining the metabolic profile of a patient (Baselt, 1996).

The techniques that are now available for the in vitro monitoring of antiretroviral drugs are time consuming, require large sample size and are relatively expensive. These techniques that are currently being used include liquid chromatography, mass spectrometry and high performance liquid chromatography. Thus there is an urgent need to develop new analytical tools that would be easy to use, capable of identifying substrates and inhibitors of an enzyme, and allow quantification of substrate turnover. The use of appropriate biosensor would be a welcome alternative, because they are generally of small size, capable of continuous measurements, and can measure analytes faster and at lower cost than traditional methods. This study reports the successful development of a nanobiosensor system on platinum surfaces using copper poly(propylene imine)–polypyrrole star copolymer coupled to CYP3A4 enzyme to determine the transformation of delavirdine.

1.4 Aim and objectives

The aim of the study was to device a copper poly (propylene imine) star copolymer nanobiosensor for the determination of delavirdine. The nanobiosensors were developed on platinum surfaces using copper poly(propylene imine)–polypyrrole star copolymer, coupled to CYP3A4 enzyme using bovine serum albumin, glutaraldehyde. The objectives of this study were as follows;

- To functionalize G2 Poly(propylene imine) (PPI) with 2 Pyrrole (PPy).
- To synthesize metallodendrimers by the incorporation of copper metal into 2-pyrrole functionalized poly (propylene imine) dendrimer.
- To characterize the G2 (Polypropylene imine)-2 Pyrrole and copper (Cu) generation-2 poly(propylene imine) to form Cu-PPI-PPy star copolymer.
- To form (Cu(G2PPI)-co-PPy)star copolymer by electropolymerisation of pyrrole onto the PPI/Pt.
- To characterize (Cu(G2PPI)-co-PPy)/Pt using CV.
- To fabricate the nanobiosesor by immobilizing CYP 3A4/BSA and Glutaraldehyde onto (Cu(G2PPI)-co-PPy).



1.5 Thesis lay-out

This thesis is presented in seven chapters

Chapter 1: Gives a brief background information on the project, the problem statement, the motivation as well as aims and objectives of this study.

Chapter 2: Provides a detailed literature review.

Chapter 3: Consists of reagents, procedures and instrumentations used to achieve the success of this study.

Chapter 4: Comprises of the results and discussion by illustrating the morphological, spectroscopic as well as electrochemical results obtained from G2 PPI-2Py, Cu-PPI-2Py and (Cu(G2PPI)-co-PPy).

Chapter 5: Provides electrochemical results obtained from the developed nanobiosensor as well as results obtained for the detection of the drug of interest.

Chapter 6: Represents conclusion and recommendations.

Chapter 7: References.



Chapter 2

Literature review



2.0 Summary

This chapter covers the role of star copolymers and their applications in the field of sensors. Dendrimers, metallodendrimers and conducting polymers and the details of their composition and properties are discussed. Cytochrome P450 enzyme family and its isoform (CYP3A4) used in this study for successful enzyme electrode formation as well as a brief description of delavirdine (an NNRTI drug) and its pharmacokinetics are also presented.

2.1 Drug metabolism

Drug metabolism is a natural progression that involves the use of the enzymatic pathways and transport systems that are the same as the one used for the metabolism of consumed food constituents. The main purpose of drug metabolism is to make the drugs more water soluble so as to allow easy excretion through urine and bile. Drugs are considered to be xenobiotics meaning that they are regarded as substances that are foreign to the body and are widely metabolised in humans. The ability to metabolize xenobiotics, while mostly beneficial, has made development of drugs very time consuming and costly due to largely (1) interindividual variations in the capacity of humans to metabolize drugs, (2) drug-drug interactions, and (3) species differences in expression of enzymes that metabolize drugs. The latter limits the use of animal models in drug development. The vast difference in metabolism of xenobiotics by different species hence animal models cannot be relied upon for the prediction and determination of the ability of humans to metabolise a drug (Cornell, 1997). Xenobiotics are metabolised by enzymes, these enzymes are commonly known as the drug-metabolising enzymes even though they are involved in the metabolism of different chemicals to which humans are exposed. Consumption or exposure to xenobiotics in the absence of metabolism will result in their accumulation in the body due to lack of efficient elimination thus resulting in toxicity (Carr, 2010).

There are three kinds of metabolizers, rapid metabolizers, slow metabolizers and intermediate metabolizers and they are characterised by their metabolic rates. Metabolic rates depend mainly on cytochrome P-450 and N-acetyltransferase enzymes. They may also differ due to drug interactions. Most commonly, this occurs when two drugs are co administered and are metabolized by the same enzyme. Patients may be classified as fast or slow metabolizers, depending on the activity levels of these enzymes. Some variants are slow metabolizers while others are ultra-rapid metabolizers. Slow metabolizers may be exposed to the active product

for longer than ultra-rapid metabolizers, or have greatly diminished exposure to the active metabolite. Conversely, ultra-rapid metabolizers risk longer exposure to the metabolite and much shorter exposure to the administered medication. Usually drug is inactivated by the P450 and poor metabolizers have higher blood level of drug and enhanced drug toxicity. It can result in loss of action of the prodrug or in toxicity due to the increase in metabolism of another pathway leading to a toxic product; as well as can have the important interactions leading to toxic response if combination of drugs metabolized by P450 is used (Crumbly, 1996).

The ideal metabolisers being the intermediate metabolisers have the ability to metabolise drugs in a normal or ideal rate. The problem with the administration of drugs is that the given dosage is ideal for the intermediate metabolisers and does not take into consideration of the rapid and slow metabolisers. The slow and ultra rapid metabolisers then stand the risk of the drug not working properly. In the case of rapid metabolisers the drugs will only be available in extremely small amounts in the blood stream and the slow metabolisers run the risk of drug toxicity due to over accumulation of the drugs in the blood stream (Ingelman-Sundberg, 2007).

There are enzymes responsible for drug metabolism and these enzymes are referred to as the drug metabolising enzymes. Majority of the metabolizing enzymes fall under the cytochrome P450 family; the enzymes of this family are capable of catalyzing the oxidative biotransformation of most drugs and other lipophilic xenobiotics. There are many enzymes found in the cytochromeP450 family but only a dozen of enzymes belonging to the 1, 2, and 3 CYP-families are responsible for the metabolism of the majority of drugs and other xenobiotics. Despite the broad and overlapping substrate specificities of these enzymes, many drugs are metabolized at clinically relevant concentrations by one or few enzymes only, which limits the important redundancy of the phase I drug oxidation system (Kirchheiner, 2007).

2.2 Delavirdine drug

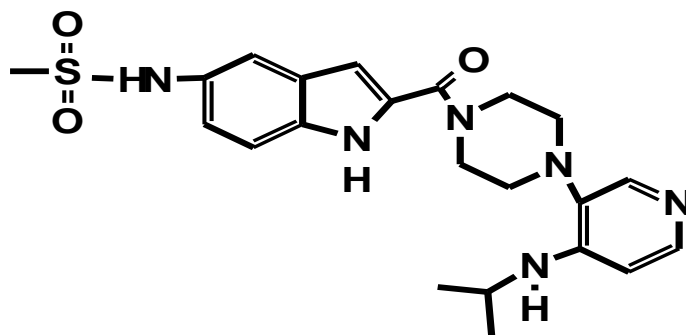


Figure 2: Structure of delavirdine

Delavirdine (brand name Rescriptor) whose structure is shown in Fig.2 is a prescription medicine used to treat HIV. It contains delavirdine mesylate (its chemical name is piperazine) a synthetic non-nucleoside reverse transcriptase inhibitor (NNRTI) of the human immunodeficiency virus. For oral administration each Rescriptor tablet contains 100-200 mg of delarvidine mesylate hence it is referred to as delavirdine (Zanger, 2013). It is converted to several inactive metabolites. It is primarily metabolised by cytochrome P4503A4, but invitro information shows that it can also be metabolised by cytochrome P4502D6. The major metabolic pathways are N-desalkylation and pyridine hydroxylation. The administration of 400 mg 3 times per day permits rapid and effective absorption of delavirdine.

The recommended dosage for Rescriptor tablets is 400 mg (four 100 mg or two 200 mg tablets) 3 times daily. Rescriptor is taken orally and can be consumed with or without food and should be used in combination with other antiretroviral therapy. The 100 mg drug can be dissolved in water whilst the 200 mg drug cannot be readily dispersed in water, thus it should be taken in its intact form. Some drugs when taken together may have interactions which may cause a defect in the functionality of the drug and impair the effects that the drug was meant to have. Delavirdine has various drug interactions with additional anti-HIV drugs which include indinavir, saquinavir and/or amprenavir which may increase with the addition of delarvidine, thus the dosage of these drugs should be attuned to compensate the interaction (Borin, 1997).

2.3 Dendrimers

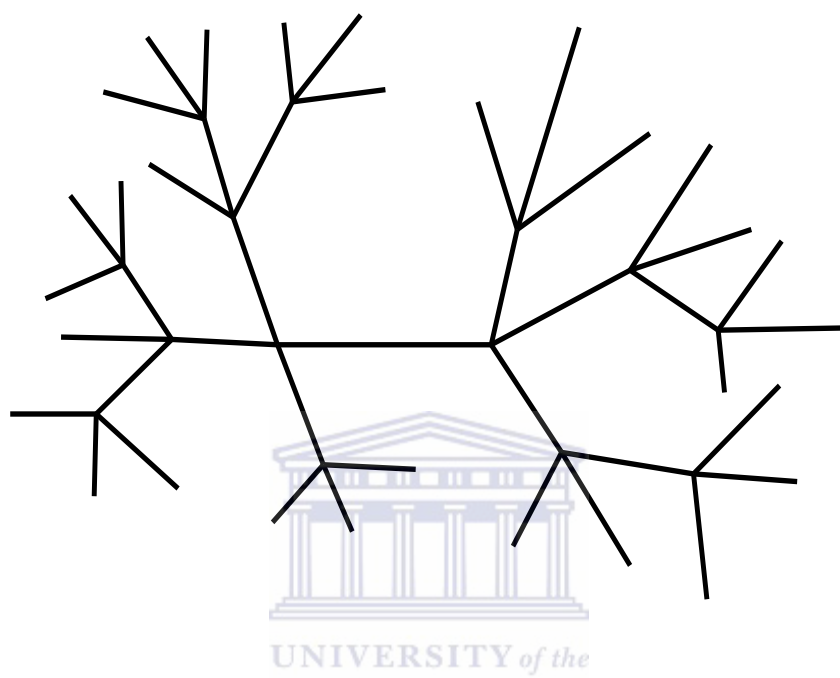


Figure 3: Hyperbranched/ tree-like structure of dendrimers

In the recent years polymer chemistry and its relative technologies had traditionally focused on linear polymers. These linear polymers rarely contain some branches ranging from short to long. It has been found that highly branched macromolecules are different in terms of properties to the conventional and well known polymers (Zolezzi, 2002). Due to their highly branched structures they have a great impact on various applications. These hyper branched molecules are termed dendrimers and were first discovered in the early 1980s by Donald Tomalia and co-workers. The term was derived from the word dendron meaning a tree in Greek as depicted in Fig.3. Dendrimers are complex macromolecules; they consist of a regular highly branched three dimensional structure. Their structure is mainly composed of 3 components, the core, the end group and branching units that link the two components. Dendrimers of lower generations (0, 1, and 2) have highly asymmetric shape and possess more open structures as compared to higher generation dendrimers. As the branching increases dendrimers tend to assume a globular structure. When they grow and thus reach a critical branched state they can no longer grow due to limited space. This phenomenon is

known as the starburst effect. The increase in dendrimer generation results in an increase in branch density. This is believed to have a major impact on the enhancement of the properties of the dendrimers. The globular shape and the presence of internal cavities make dendrimers possess unique properties. The most important of these unique properties is the possibility to encapsulate guest molecules in the macromolecular interior.

Dendrimers are classified by the generation number which is the number of repeated branching of the dendrimers. Dendrimers are produced in iterative reaction steps, in which each additional iterative step results in a higher generation dendrimer. Their synthesis is one of the examples of controlled hierarchical synthesis using specifically-designed chemical reactions. Each successive generation results in double the number of end groups (active sites) and with approximately twice as much molecular weight than the previous generation. The application of dendrimers in electrochemical biosensors is an emerging area of research. The structural homogeneity, biocompatibility, internal porosity, high surface area and ease of functionalization of dendrimers make them very desirable for biosensor applications (Klajnert, 2001).

2.3.1 Types of dendrimers

2.3.1.1 Poly (Propylene imine) dendrimers

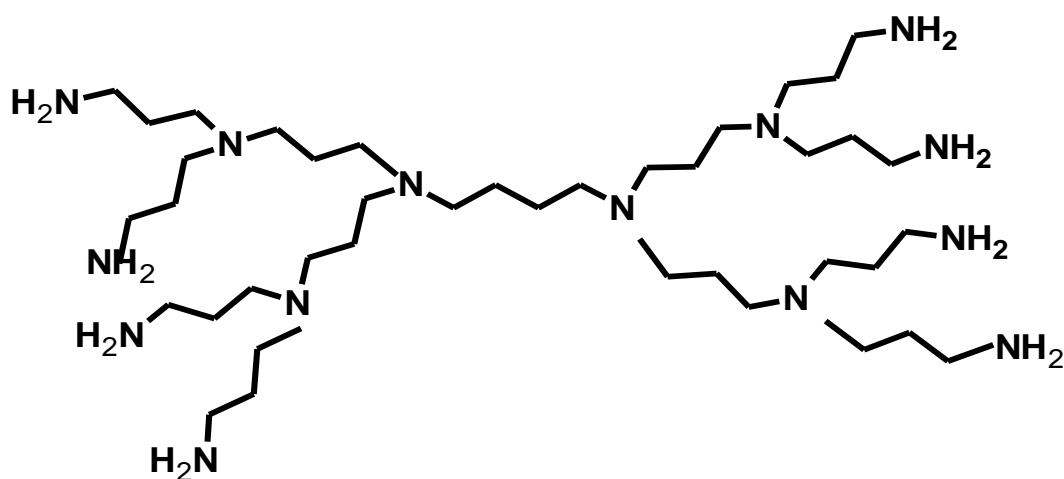
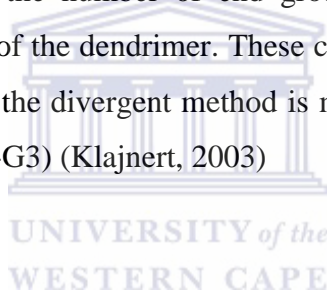


Figure 4: Structure of PPI dendrimer

Poly(Propylene imine) (PPI) dendrimers are generally poly-alkylamines consisting of primary amines as the end groups, while the interior of the dendrimer consists of a number of tertiary tris-polypropylene amines. The nitrogen atoms serve as the branching points of the dendrimer. An alternative name that is occasionally used to describe this class of PPI dendrimers is Poly (Propylene amine) (POPAM) (Newkome, 2007). They are also referred to as DAB-dendrimers due to the fact that the core structure is usually based on diamino butane. PPI dendrimers are available commercially but up to 5 generations. They can be synthesised by the divergent method. In the divergent approach the building up of the dendrimer takes place in a step wise manner starting from the core and building up the molecule towards the periphery using two basic methods (1) coupling of the monomer and (2) the deprotonation or transformation of the monomer end group which creates a new reactive surface functionality. The synthesis of PPI dendrimer using the divergent methods shows some defects when synthesising PPI dendrimers of higher generations (G4-G5). Higher generations are characterised by an increase in the number of end groups to be functionalised and the increase in the molecular weight of the dendrimer. These characteristics make their synthesis very difficult. The application of the divergent method is most successful in the synthesis of lower generation dendrimers (G1-G3) (Klajnert, 2003)



2.3.1.2 Metallodendrimers

The study of metals coordinated onto dendrimer structures dates back to the year 1992. This coordination of metal onto dendrimers generates what is known as metallodendrimers. The introduction of metal centers may occur at various branching points within the dendrimers, at the core or on the periphery of the dendritic molecule. Metals have played a significant role in the synthesis of other, non-dendritic supramolecular structures, and thus their potential applicability in the construction of metallodendrimers was evident (Gorman, 1998). The incorporation of metals onto dendrimer structures has resulted in materials/molecules with enhanced and potentially useful properties. Metals have played an important role in the synthesis of other supramolecules other than dendrimers. They have been used in the enhancement of the properties of those molecules and thus their potential in their application in the construction of the metallodendrimers was evident. Due to their altered properties metallodendrimers have various application potential such as their use in the fields of catalysis where dendrimers have been employed as multi-centred catalysts. It has been

determined that relatively high molecular weight metallodendrimer catalysts could have the potential to be easily precipitated from a reaction and recycled. They are also applied in sensing where they can influence the microenvironment around a redox centre and thus sterically mediate the transfer of electrons (Barner-Kowollik, 2006).

2.4 Polymers

2.4.1 Conducting polymers

Conducting polymers typically contain as the fundamental structural unit, a linear backbone of repeating conjugated monomers (Bhakshi, 2004). Conductive polymers were initially made in 1930 for the purpose of preventing corona discharge. The potential uses for conductively filled polymers have since been multiplied due to their ease of processing, good environmental stability and wide range of electrical properties. Over the past 25 years various conjugated polymers have been synthesized which exhibit excellent electrical properties (Skotheim, 1986). Owing to the delocalization of electrons in a continuously overlapped S-orbital along the polymer backbone, certain conjugated polymers also possess interesting optical and magnetic properties. These unusual optoelectronic properties allow conjugated polymers to be used for a large number of applications, including protecting metals from corrosion, sensing devices, artificial actuators, all-plastic transistors, non-linear optical devices, light-emitting displays, electrocatalysis, rechargeable batteries, membrane separation, optoelectronic, chromatography; solar cells (Ahuja, 2007; Malholtra, 2006) and most recently they have found great application in electrochemical biosensors. This is attributed to properties namely mechanical flexibility, chemical specificities, tunable conductivities, high surface areas and easy processing (Ramakrishnan, 1997).

2.4.1.1 Polypyrrole

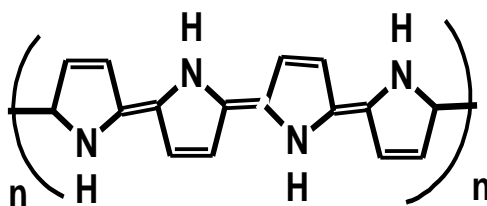


Figure 5: Structure of polypyrrole

Polypyrrole is one of the extensively studied conducting polymers. It is a chemical compound that is formed from a number of connected pyrrole ring structures (Fig.5). It is an inherently conductive polymer due to interchain hopping of electrons. Polypyrrole is easy to prepare by electrochemical techniques and its surface charge characteristics can easily be modified by changing the dopant anion that is incorporated during synthesis (Brezoi, 2010). Polypyrrole was the first of conducting polymers that shows relative high conductivity. Conducting polymer can be synthesised electrochemically or chemically. Polypyrrole can be obtained through cationic radical, electrochemically or vapour phase polymerization. Among these methods cationic radical is the only way of producing high quantity massive conducting polymers and is the most promising in industrial applications. Polypyrrole is mainly synthesised electrochemically since it is the simplest method it is a quicker and more controllable method in comparison to the chemical method (Zhou, 1999). Pyrrole is polymerized through the oxidation of the pyrrole monomer through a pseudo poly condensation process. Of all the conducting polymers polypyrrole is the most interesting due to the fact that it is easily deposited from aqueous and non-aqueous media, very adherent to many types of substrates, and is well-conducting and stable. As a result of its electroactivity, high electrical conductivity and stability it is frequently used in commercial applications such as sensors, batteries, molecular devices and membranes (Sadki, 2000).

2.4.1.2 Electrochemical polymerization of pyrrole

During electrochemical polymerization, the monomer, dissolved in an appropriate solvent containing the desired anionic doping salt, is oxidized at the surface of an electrode by application of an anodic potential (oxidation). The choice of the solvent and electrolyte is of particular importance in electrochemistry since both solvent and electrolyte should be stable at the oxidation potential of the monomer and provide an ionically conductive medium. Since pyrrole has a relatively low oxidation potential, electropolymerization can be carried out in aqueous electrolytes which is not possible for thiophene or benzene (Zhou, 1999). As a result of the initial oxidation, the radical cation of the monomer is formed and reacts with other monomers present in solution to form oligomeric products and then the polymer. The extended conjugation in the polymer results in a lowering of the oxidation potential compared to the monomer. Therefore, the synthesis and doping of the polymer are generally done simultaneously (Sadki, 2000). The anion is incorporated into the polymer to ensure the electrical neutrality of the film and, at the end of the reaction a polymeric film of controllable thickness is formed at the anode. The anode can be made of a variety of materials including platinum, gold, glassy carbon, and tin or indium–tin oxide (ITO) coated glass. The electropolymerization is generally achieved by potentiostatic (constant potential) or galvanostatic (constant current) methods. These techniques are easier to describe quantitatively and have been therefore commonly utilized to investigate the nucleation mechanism and the macroscopic growth. Potentiodynamic techniques such as cyclic voltammetry correspond to a repetitive triangular potential waveform applied at the surface of the electrode. The latter method has been mainly used to obtain qualitative information about the redox processes involved in the early stages of the polymerization reaction, and to examine the electrochemical behaviour of the polymer film after electrodeposition.

2.4.1.3 Star copolymers

In recent years, focus on electronically conducting polymers has increased in the wake of their large number of potential applications emerging in the market, such as in the case of light-emitting diodes, electrochemical supercapacitors, sensors, batteries, memory-storage devices, electrochromic displays, nonlinear circuit elements and ion gates (Park, 2013). Recently the research focus has shifted to the copolymerization to prepare conducting

polymers with better properties (properties of both the polymer) and to overcome limitations of the variety of new monomers. By applying the proposed electrochemical copolymerization, new conducting copolymers have been prepared with pronounced and clear advantages in term of enhanced electrochemical property, thermal and environmental stability (Gupta, 2014). Star copolymers can be defined as a class of branched macromolecules that have a central core to which multiple linear polymer chains are attached. The 3D structure with extended conjugated linear polymer chains give star copolymers properties that are different from the typical 2D, linear polymers. The combination of star copolymer and conducting polymer structures open up an approach to making materials that have the favourable properties of both, i.e., improved processability and electrical conductivity. Improved process ability results from the spheroidal structure of hyperbranched, dendrimeric and starburst polymers (Ottaviani, 1994).

2.5 Biosensors

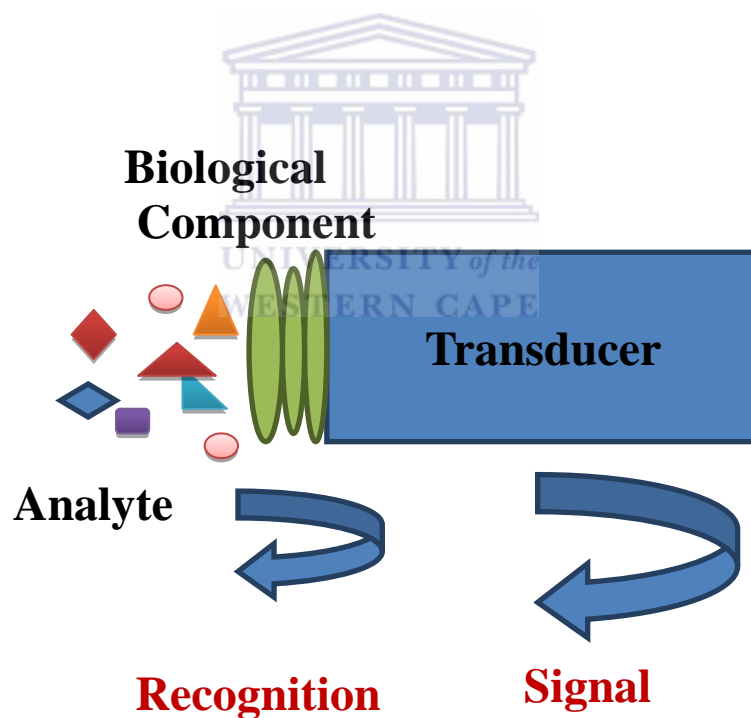


Figure 6: Biosensor components

The most widely accepted definition of biosensors is it is a self-contained analytical device that incorporates a biologically active material in direct contact with an appropriate

transduction element for the purpose of detecting (reversibly and selectively) the concentration or activity of chemical species in any type of sample (Wang, 1996). A biosensor consists of three components, namely, the sensitive **biological element**, the **transducer** and the **signal processor** (Fig.6). The sensitive **biological element** (e.g enzymes, nucleic acids, nucleic acids etc) is a biologically derived material or biomimetic component that interacts with the analyte under study by recognizing and binding onto it. A typically biosensor consists of a bio-recognition component, biotransducer component, and electronic system which include a signal amplifier, processor, and display (Pan, 2007). The component that is responsible for the recognition of the analyte, called a bioreceptor, utilizes biomolecules from organisms or receptors modeled after biological systems to interact with the analyte of interest. This interaction is measured by the biotransducer which outputs a measurable signal that is proportional to the amount of the target analyte present in the sample. The idea behind the design of a biosensor is to facilitate quick, convenient testing at the point of concern or care where the sample was procured (Pohanka, 2008).

The sole mandate of the bioreceptor is to facilitate an interaction with the specific analyte of interest that can be measured by the receptor. The analyte of interest is often found amongst a matrix of other chemical or biological components. The type of biomolecule employed varies depending on the analyte of interest, thus biosensors can be classified based on bioreceptor interactions, e.g. Antibody/antigen, enzymes, nucleic acids/DNA (Cornell, 1997).

2.5.1 Electrochemical biosensors

Electrochemical biosensors have been the subject of research for almost five decades. The principle of the first enzyme electrode immobilised with glucose oxidase was introduced by Leland Clark in the year 1962 at the New York Academy of Sciences Symposium. The most typical part of electrochemical biosensors is the presence of a suitable enzyme in the biorecognition layer providing electroactive substances for detection by the physico-chemical transducer providing the measurable signal. A native enzyme can be used as the biorecognition component; in this case the analyte is equal to the enzyme substrate; alternatively it may function as its inhibitor. In addition, enzymes can be used as labels bound to antibodies, antigens and oligonucleotides with a specific sequence, thus providing affinity-based sensors. Based on their operating principle, the electrochemical biosensors can employ potentiometric, amperometric and impedimetric transducers converting the chemical

information into a measurable amperometric signal (Pohanka, 2008). Biosensors are categorized according to the basic principles of signal transduction and biorecognition elements. According to the transducing elements, biosensors can be classified as electrochemical, optical, piezoelectric, and thermal sensors. Electrochemical biosensors are also classified as potentiometric, amperometric and conductometric sensors (Kerman, 2004).

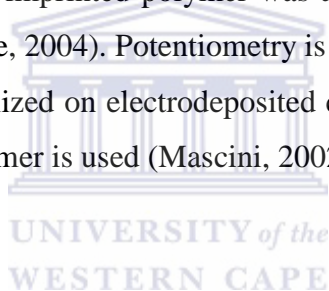
2.5.1.1 Amperometric biosensors

Amperometric biosensors are quite sensitive and more suited for mass production than the potentiometric ones. Amperometric biosensors can work in two- or three-electrode configurations. The former case consists of reference and working (containing immobilized biorecognition component) electrodes. The main disadvantage of the two-electrode configuration is limited control of the potential on the working electrode surface with higher currents, and because of this, the linear range could be shortened. To solve this problem, a third auxiliary electrode is employed. Now voltage is applied between the reference and the working electrodes, and current flows between the working and the auxiliary electrodes. The working electrode of the amperometric biosensor is usually either a noble metal or a screen-printed layer covered by the biorecognition component (Liepold, 2005). Amperometric biosensors are based on the monitoring of the electron transfer processes that take place. The signal of these biosensors is generated through the electron exchange that occurs between the biological system and the electrode. On amperometric biosensors the analyte undergoes a redox reaction followed by the measurement of the current in an electrochemical cell. The analyte, or the species involved with it via a (bio) chemical reaction, changes its oxidation state at one electrode. The electron flux is then monitored and is proportional to the amount of the species electrochemically transformed at the electrode (Belluzo, 2008). The amperometric biosensors are often used on a large scale for analytes such as glucose, lactate (Ohnuki et al. 2007), and sialic acid (Marzouk, 2007).

2.5.1.2 Potentiometric biosensors

Potentiometric biosensors are based on ion-selective electrodes (ISE) and ion-sensitive field effect transistors (ISFET). The primary outputting signal is possibly due to ions accumulated

at the ion-selective membrane interface (Belluzo, 2008). Current flowing through the electrode is equal to or near zero. The electrode follows the presence of the monitored ion resulting from the enzyme reaction (Kauffmann, 1991). Nowadays, semi conductor based physico-chemical transducers are more common. ISFETs and light addressable potentiometric sensor (LAPS) based systems especially are convenient for biosensor construction. The ISFET principle (Yuqing, 2003) is based on a local potential generated by surface ions from a solution. The LAPS principle (Yoshinobu, 2005) is based on semiconductor activation by a light-emitting diode (LED). The sensor is made from an n-type silicon typically coated with 30 nm of silicon oxide, 100 nm of silicon nitride, and indium-tin oxide. The LAPS measures a voltage change as a function of medium pH in the LED activated zone. This opens the way for multiposition sensing and construction of an array of biorecognition zones. A potentiometric biosensor with a molecularly imprinted polymer constructed for the herbicide atrazine assay allows detecting from 3×10^{-5} to 1×10^{-3} M (D'Agostino, 2006); molecularly imprinted polymer was also used for tracking the level of neurotransmitter serotonin (Kitade, 2004). Potentiometry is rarely used in biosensing methods especially with enzymes immobilized on electrodeposited conducting polymers in which pH sensitivity of the conducting polymer is used (Mascini, 2002).



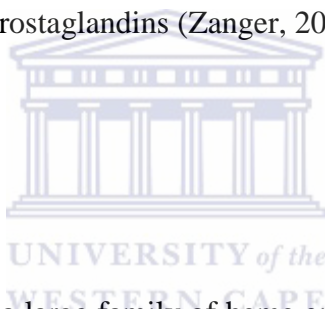
2.5.1.3 Impedimetric biosensors

Such devices follow either impedance (Z) or its components resistance (R) and capacitance (C); inductance typically has only a minimal influence in a typical electrochemical setup. The inverse value of resistance is called conductance and for this reason some investigators name such systems as conductometric. Impedance biosensors include two electrodes with applied alternating voltage; amplitudes from a few to 100 mV are used. The impedance biosensor is commonly a functional part of the Wheatstone bridge. These systems are considered for the assay of urea when urease is used as a biorecognition component. Alternatively, impedance biosensors have been successfully used for microorganism growth monitoring due to the production of conductive metabolites (Silley, 1996). The main disadvantage of impedance biosensors is that they give false positive results due to electrolytes from the samples. Impedimetric biosensors are less frequent compared to potentiometric and amperometric biosensors; nevertheless, there have been some promising

approaches. Hybridization of DNA fragments previously amplified by a polymerase chain reaction has been monitored by an impedance assay (Belluzo, 2008).

2.6 Enzyme

Enzymes are proteins that possess high catalytic activity and selectivity towards substrates. They have been used for decades to assay the concentration of diverse analytes (Pohanka, 2008). Their commercial availability at high purity levels makes them very attractive for mass production of enzyme sensors. Their main limitations are that pH, ionic strength, chemical inhibitors, and temperature affect their activity. Most enzymes lose their activity when exposed to temperatures above 60.8°C. Drug metabolizing enzymes are a group of different proteins; they are responsible for the metabolism of a vast different number of xenobiotic compounds which includes drugs, environmental pollutants and endogenous compounds such as steroids and prostaglandins (Zanger, 2013).



2.6.1 Cytochrome P450

Cytochrome P450 (CYP) is from a large family of heme enzymes that catalyze a diversity of chemical reactions such as epoxidation, hydroxylation and heteroatom oxidation. The hepatic CYP are a multigene family of enzymes that play a vital role in the metabolism of many drugs and xenobiotics with each cytochrome isozyme responding differently to exogenous chemicals in terms of its induction and inhibition. Their catalytic ability has attracted a lot of interest of enzyme engineers since the 1970's (Bistolos, 2005). Only about a dozen enzymes belonging to the 1, 2, and 3 CYP-families are responsible for the metabolism of the majority of drugs and other xenobiotics. Despite the broad and overlapping substrate specificities of these enzymes, many drugs are metabolized at clinically relevant concentrations by one or few enzymes only. The CYP1 family consists of three functional genes in two subfamilies. The highly conserved CYP1A1 and CYP1A2 genes consist of seven exons and six introns and are located on chromosome 15q24.1, whereas CYP1B1 consists of only three exons located on chromosome 2p22.2 (Zanger, 2013). Catalytic activities of the CYP1 enzymes are overlapping and include hydroxylations and other oxidative transformations of many polycyclic aromatic hydrocarbons and other aromatic substances. Whereas CYP1A1 prefers

planar aromatic hydrocarbons, CYP1A2 shows a preference for aromatic amines and heterocyclic compounds. Due to its relatively high expression in liver, CYP1A2 plays a significant role in the metabolism of several clinically important drugs. These include analgesics and antipyretics (acetaminophen, phenacetin, lidocaine), antipsychotics, antidepressants, anti-inflammatory drugs, cardiovascular drugs (propranolol, guanabenz, triamterene), the cholinesterase inhibitor tacrine used for the treatment of Alzheimer's disease, the muscle relaxant tizanidine. The CYP2 family contains 16 full-length genes, which all have 9 exons and 8 introns. Several of the most important hepatic drug metabolizing CYPs but also extrahepatic enzymes and several “orphan” P450s with still unclear function are found in this family. The genes are spread over different chromosomes and organized in multi-gene clusters containing one or several subfamilies. Most pharmacologically important CYP2 genes are highly polymorphic, in particular CYP2A6, CYP2B6, CYP2C9, CYP2C19, and CYP2D6.

The human CYP3 family consists only of one subfamily, CYP3A, which is located on chromosome 7q22.1. In humans, there are four CYP3A genes namely CYP3A4, CYP3A5, CYP3A7, and CYP3A43. CYP3A4 is expressed at high levels in adult liver and small intestines. The CYP3A drug-metabolizing enzymes facilitate the metabolism and elimination of a wide range of structurally different xenobiotics and of 50% of all therapeutic drugs used in the clinics (Ingelman-Sundberg, 2007). CYP3A4 is the major expressed P450 in intestinal enterocytes, with levels uncorrelated to those of liver, and contributes substantially to the first-pass metabolism of orally administered drugs (Zanger, 2013). In this study CYP3A4 enzyme was used as a bio-component in developed electrochemical sensor for delavirdine drug.

2.6.2 Mechanism of CYP450 Enzyme complex

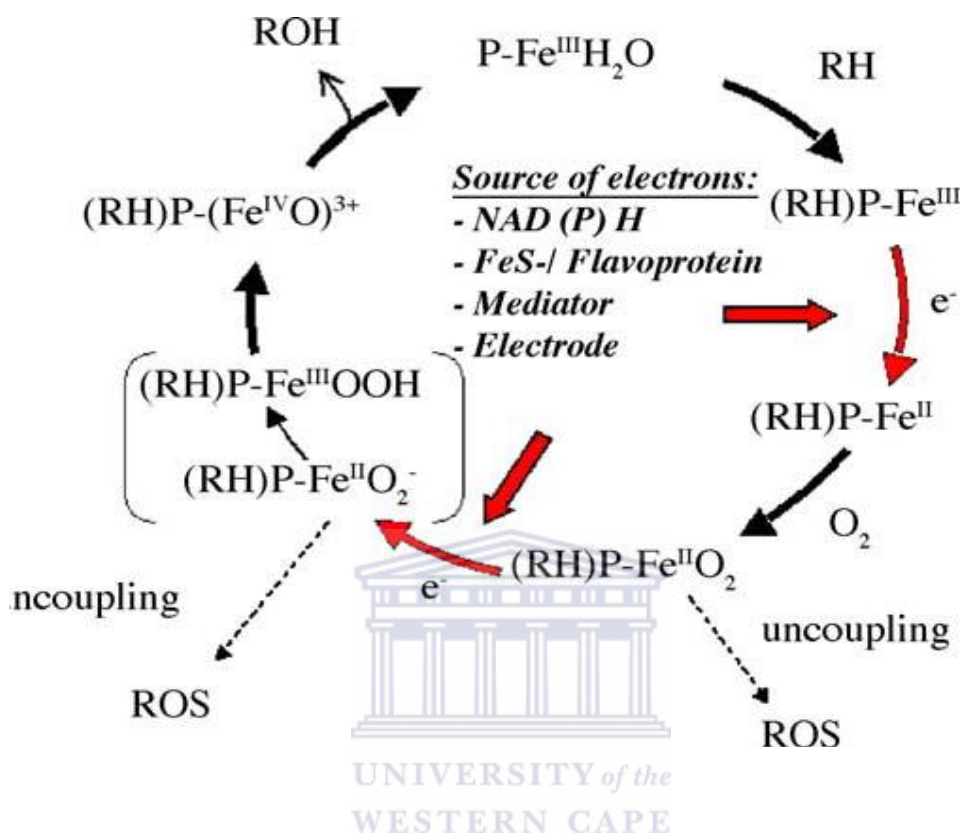


Figure 7: Catalytic cycle of CYP

The P450 catalytic cycle (Fig.7) shows the steps involved when a substrate binds to the enzyme in the normal state of a P450 with the iron in its ferric $[\text{Fe}^{3+}]$ state. When the substrate binds to the enzyme, the enzyme is reduced to the ferrous $[\text{Fe}^{2+}]$ state by the addition of an electron from NADPH cytochrome P450 reductase. The bound substrate facilitates this process. Molecular oxygen binds and forms a Fe^{2+}OOH complex with the addition of a proton and a second donation of an electron from either NADPH cytochrome P450 reductase or cytochrome b5. A second proton cleaves the Fe^{2+}OOH complex to form water. An unstable $[\text{FeO}]^{3+}$ complex donates its oxygen to the substrate. The oxidised substrate is released and the enzyme returns to its initial state. The active site of cytochrome P450 contains a heme iron center. The iron is tethered to the P450 protein via a thiolate ligand derived from acysteine residue. This cysteine and several flanking residues are highly conserved in known CYPs enzyme complex

Chapter 3

Experimental methods



3.0 Summary

This chapter describes the procedures for the synthesis of G2PPI-2Py and (Cu(G2PPI)-co-PPy using appropriate reagents. This chapter contains the immobilization procedure used to attach the enzyme for the development of biosensor. Also included in the chapter are the characterization procedures for the biosensors as well as other materials used towards the fabrication of the biosensors using various techniques; spectroscopic (FTIR) and (EDS), microscopic (HRSEM, HRTEM) and electrochemical Cyclic voltammetry (CV).

3.1 Reagents

Pyrrole-2-carboxy aldehyde (98%), dichloromethane (98%), methanol (>99.9%), copper acetate monohydrate (99.99%) and generation 2 poly(propylene imine) dendrimer were purchased from Sigma Aldrich while ethanol 96.4% purchased from Kimix were used for the preparation of copper metalodendrimer. Electropolymerization was achieved by the use of reagent grades pyrrole (98%) and lithium per chlorate (99.9%) were purchased from Sigma Aldrich. The reaction medium, pH 7.4, 0.1 M phosphate buffer was prepared from sodium phosphate dibasic dihydrate ($\text{HNa}_2\text{O}_4\text{P}\cdot 2\text{H}_2\text{O}$) ($\geq 99.5\%$) and sodium phosphate monobasic dihydrate ($\text{H}_2\text{NaO}_4\text{P}\cdot 2\text{H}_2\text{O}$) ($\geq 99\%$) that were purchased from Sigma Aldrich. Immobilisation reagents such as grade I 25% glutaraldehyde was purchased from Sigma Aldrich while bovin serum albumin (BSA) was purchased from Fluka. Cytochrome P450-3A4 (CYP3A4) human expressed in *Saccharomyces cerevisiae* was purchased from Sigma Aldrich. The nanobiosensor substrate deavidine mesylate was purchased from Sigma alridch. Alumina micro polishing pads were obtained from Buehler LL, USA. De-ionized ultra-purified water used throughout these experiments was prepared with a Milli-Q water purification system.

3.2 Intsrumentation

All electrochemical measurements were done using BASi epsilon from Bio Analytical Systems (BAS), Lafayette, USA.

All cyclic voltammograms were recorded with computer interfaced to BASi epsilon using a 10 mL electrochemical cell with a three electrodes set up. The electrodes used in the study were (1) Platinum working electrode ($A = 0.0201 \text{ cm}^2$) from BAS, (2) platinum wire from

Sigma Aldrich acted as counter electrode and (3) Ag/AgCl from BAS kept in (3 M NaCl) was the reference electrode and alumina micro polishing pads were obtained from Buehler, LL, USA and were used for polishing the platinum working electrode before modification. HRTEM images were taken using Tecnai G2 F20X-Twin MAT 200kV Field Emission Transmission Microscopy from FEI (Eindhoven, Netherlands). All FTIR spectra were recorded on spectrum 100 FTIR spectrometer (PerkinElmer, USA) in a region of 400 to 4000 cm^{-1} . All samples were dried using Buchi rotarvapor and buchi waterbath from labotech at 60⁰C.

3.2.1 Spectroscopic techniques

3.2.1.1 Fourier transform infra-red spectroscopy (FTIR)

Infrared spectroscopy is one of the most important analytical techniques available to today's scientists. Infra-red spectroscopy is the study of the interaction and relationship between matter and electromagnetic fields in the infra red region. It is a powerful tool that provides information about the chemical composition of a sample. One of the great advantages of infrared spectroscopy is that virtually any sample in virtually any state may be studied. Liquids, solutions, pastes, powders, films, fibres, gases and surfaces can all be examined with a judicious choice of sampling technique. As a consequence of the improved instrumentation, a variety of new sensitive techniques have now been developed in order to examine formerly intractable samples (Stuart, 2004). In the study it was used for the determination of the chemical compositions of (Cu(G2PPI-2Py) metallodendrimer and G2PPI-2Py and to identify the types of interactions present in the complexes.

3.2.1.2 Energy dispersive spectroscopy (EDS)

Energy Dispersive Spectroscopy (EDS) makes use of the X-ray spectrum emitted by a solid sample bombarded with a focused beam of electrons to obtain a localized chemical analysis. All elements from atomic number 4 (Be) to 92 (U) can be detected in principle, though not all instruments are equipped for 'light' elements ($Z < 10$). Qualitative analysis involves the identification of the lines in the spectrum and is fairly straightforward owing to the simplicity of X-ray spectra. Quantitative analysis (determination of the concentrations of the elements present) entails measuring line intensities for each element in the sample and for the same elements in calibration Standards of known composition (Ramamurthy, 2009). In this study

EDS was used for the determination of the presence of the copper element in G2PPI-2Py and (Cu(G2PPI-2Py)) respectively. It was determined that copper was present in the (Cu(G2PPI-2Py)) but not in G2PPI-2Py, signifying successful incorporation of copper nanoparticles.

3.2.2 Microscopic techniques

3.2.2.1 High resolution transmission electron microscopy (HRTEM)

High resolution Transmission electron microscopy uses a series of electromagnetic lenses for the manipulation of an electron beam generated at a high potential in an electrically heated filament. In HRTEM the image and corresponding diffraction pattern from the same part of the sample, the concentration of the elements in the sample as well as the mapping of the elements in the same region of the sample can be obtained through the analysis of the image and the corresponding diffraction useful information can be obtained about the grain size, precipitates and their orientation on the matrix and on the appearance of the superstructure (Tonejc, 1999). In this study HRTEM was used to determine the particle size and shape of the copper nanoparticles that was incorporated into the dendrimer which were determined to be 12-17 nm and spherical in shape.

3.2.2.2 High resolution scanning electron microscopy (HRSEM)

High resolution scanning electron microscopy is a microscopic technique that uses the interaction between an electron beam and the atoms of the targeted sample to generate an image through the emission of different signals (Sun, 2007). The general principle essential to electron microscopy techniques is the interaction between an electronic beam and the atoms of a target sample. In HRSEM, a high-energy, very thin electron beam is finely focused over a sample and swept in a raster across the surface. The electron beam and sample interactions cause the emission of different signals, which are collected by specific detectors and converted into an image of the sampled area. The signals generated include secondary electrons. The signals of greatest interest for surface topography are secondary and backscattered electrons. The characteristic X-rays, emitted as a result of electron bombardment, are element specific and permit both qualitative and quantitative elemental analysis in electron probe microanalysis (Marassi, 2009). In the study it was used for the

determination of the surface morphologies of G2PPI-2Py and (Cu(G2PPI-2Py) metallodendrimer and to determine whether there was any change in the morphology after introduction of copper nano particles. Where the SEM of G2PPI-2Py showed a rough surface and that of (Cu(G2PPI-2Py) after copper incorporation.

3.2.3 Electrochemical techniques

3.2.3.1 Cyclic Voltammetry (CV)

Cyclic voltammetry is the most widely used technique for acquiring qualitative information about electrochemical reactions. Is a technique that is mostly used to acquire qualitative information about electrochemical reactions that occur. It offers a rapid location of redox potentials of the electroactive species (Andrienko, 2008). This technique can be used to get valuable kinetic information of electrode reaction. Electrode reaction usually involves electron transfer reaction which is influenced by electrode potential. Voltammetry is used to investigate electrode mechanism. Advantages of this technique include its broad accessibility due to its low cost and the accessibility to extensive theory for electrochemist as well as other field of specialists. However this technique has some drawbacks which include the difficulty to determine the mechanism of the second of two or more closely spaced charge transfer reactions (Nicholson, 1965). In this study CV was used to determine the electrochemical activity of (Cu(G2PPI)-co-PPy) and G2PPI-2Py whereby there was an observed increase in current with an increase in applied potential and was used for the testing of the biosensor and determination of the analyte of interest.

3.3 Methodology

3.3.1 Synthesis of 2-Pyrrole functionalized Poly(propylene imine) dendrimer (PPI-2Py)

The synthesis of G2PPI-2Py was carried out by, first, a condensation reaction of PPI with Pyrrole-2- carboxy aldehyde. A reaction mixture of PPI generation 2 (1 g, 3.15 mmol) and pyrrole-2- aldehyde (1.2 g, 12.625 mmol) in 50 ml dry methanol the mixture was magnetically stirred under a positive pressure of nitrogen gas for 2 d in a 100 ml three-necked round bottom flask. Methanol was removed by rotary evaporation, the residual oil was dissolved in 50 ml dichloromethane (DCM), and the organic phase was then washed with water (6×50 ml) to remove unreacted monomer. The DCM was removed by rotary evaporation and the desired product was an orange oil (Baleg, 2011).

3.3.2 Synthesis of generation 2 copper metallodendrimer

Cu (OAc)₂ · H₂O (1mmol) and G2PPI-2Py (0.25mmol) were mixed in 20 ml methanol. The mixture was refluxed for 4h yielding a green precipitate. The mixture was cooled to 0°C and the mixture was filtered under vacuum and dried in the oven at 300°C. The product was recrystallized from 1:2 dichloromethane/ethanol mixture at -4°C for 72 h (Mapolie, 2013).

3.4 Pre-treatment of working electrode

A platinum working electrode was polished with 1, 0.5 and 0.03 μm alumina slurries in polishing pads, minimum of 5 min on each pad, after polishing, the electrode was ultrasonicated for 15 min, with distilled water and absolute ethanol respectively to remove any possibly adsorbed alumina crystals on the electrode surface and rinsed carefully with distilled water. The above procedure resulted into a clean platinum working electrode.

3.4.1 Electrochemical polymerization of pyrrole on Pt electrode

Electrochemical polymerization of Py on Pt electrode surfaces coated with G2PPI-2Py was carried out in an electrochemical cell containing 5 mL of 0.1 M aqueous lithium perchlorate solution as support electrolyte and 75 μL of Py monomer. Electrochemical polymerization

was achieved by CV (+800 mV to -800 mV), performed at a scan rate of 50 mV/s, for 30 cycles. Before applying the potential to the above polymerization solution, the solution was degassed by bubbling argon gas through for 15 min, and then maintaining it oxygen-free by keeping a blanket of argon above the solution. Oxygen was removed to ensure that it did not interfere with the electronic processes that takes place on the surface of the electrode. It is during this electropolymerization process that PPy is electrodeposited on the surface of the coated electrode. The modified electrode (PPy/PtE) was then removed from the solution and rinsed with water to remove any traces of monomer.

3.4.2 Electrochemical polymerization of Pyrrole on Pt electrode surface coated with G2Cu-PPI-2Py

3 μ L G2Cu-PPI-2Py was drop-coated onto platinum working electrode and dried for 4 h. Electrochemical polymerization of Py on Pt electrode surfaces coated with G2PPI-2Py was carried out in an electrochemical cell containing 5 mL of 0.1 M aqueous lithium perchlorate solution as support electrolyte and 75 μ L of Py monomer. Electrochemical polymerization was achieved by CV (+800 mV to -800 mV), performed at a scan rate of 50 mV/s, for 30 cycles. Before applying the potential to the above polymerization solution, the solution was degassed by bubbling argon gas through for 15 min, and then maintaining it oxygen-free by keeping a blanket of argon above the solution. It is during this electropolymerization process that PPy is electrodeposited on the surface of the coated electrode. The modified electrode (Cu(G2PPI)-co-PPy) was then removed from the solution and rinsed with water to remove any traces of monomer.

3.4.3 Fabrication of biosensors

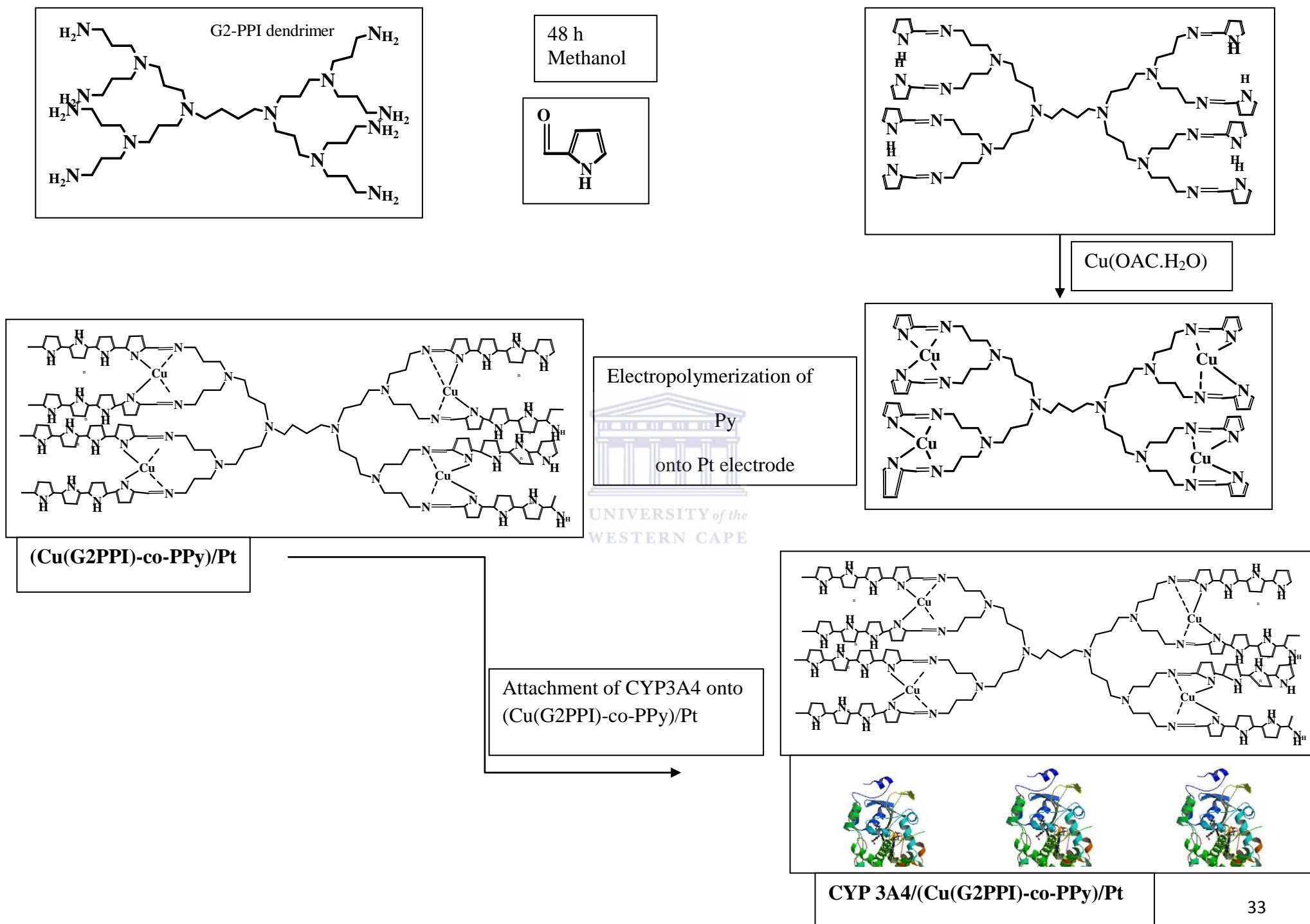


Figure 8: Schematic representation for development of CYP3A4/(Cu(G2PPI)-co-PPy)/Pt

3.4.3.1 Fabrication of CYP3A4 biosensor: CYP/Pt

3 μL of a 1M CYP enzyme solution, containing 2.0 mg BSA and CYP3A4 was carefully drop-coated onto clean Pt electrode. 2 μL 2.5% glutaraldehyde solution was drop-coated onto platinum working electrode containing CYP3A4 and BSA solution. The CYP3A4 modified electrode was covered in a tight fitting lid for first 10 min to allow the formation of a uniform layer, the lid was removed and the enzyme was allowed to dry for 4 h at 4°C. The resulting electrode was rinsed with 0.1 M PBS pH 7.4 to remove any physically adsorbed enzyme. The CYP3A4-based biosensor was denoted CYP3A4/Pt and was kept at 4°C in 0.1M PBS pH 7.4 when not in use.

3.4.3.2 Fabrication of CYP 3A4 biosensor: (Cu(G2PPI)-co-PPy)/BSA/Glu/Pt

CYP3A4 was immobilized on the (Cu(G2PPI)-co-PPy)/Pt by drop-coating. 3 μL of a 1M enzyme solution, containing 2.0 mg BSA and CYP3A4 was carefully drop-coated onto the Cu-PPI-PPy modified Pt electrode. 2 μL 2.5% glutaraldehyde solution was drop-coated onto modified electrode. The enzyme-modified electrode was then covered with a tight fitting lid for the first 10 min to form a uniform layer, after which, the lid was removed and the enzyme layer was slightly dried for another 40 min, but still retaining wet camera (wet camera consisting of CYP3A4, glutaraldehyde and BSA) after which the prepared biosensor was immediately placed at 4°C for at least 1h. The CYP3A4-based biosensor was denoted CYP 3A4/ (Cu(G2PPI)-co-PPy)/Pt.

3.5 Preparation of Delavirdine stock

5 mg of powder delavirdine drug was placed in a 100 ml volumetric flask which was filled up to the mark with 0.1 M sodium phosphate buffer solution, pH 7.4. Un-dissolved components were removed by filtering the formed suspension through a Whatman polytetrafluoroethylene 35 syringe filter (pore size 0.3 μm) into a clean storage bottle and the concentration of prepared delavirdine was found to be 100 μM . The solution was used as stock delavirdine solution from which all the other working solutions were prepared using appropriate dilutions with 0.1 M sodium phosphate buffer pH 7.4.

Chapter 4

Results and discussion



4.0 Summary

This chapter deals with the characterisation of G2PPI-2Py and (Cu(G2PPI-2Py)) using FTIR, HRSEM, HRTEM and EDS. Also included in this chapter is the electrochemical investigation and properties of PPy and Cu-PPI-PPy using CV.

4.1 Spectroscopic characterisation of G2 PPI-2Py and (Cu(G2PPI-2Py))

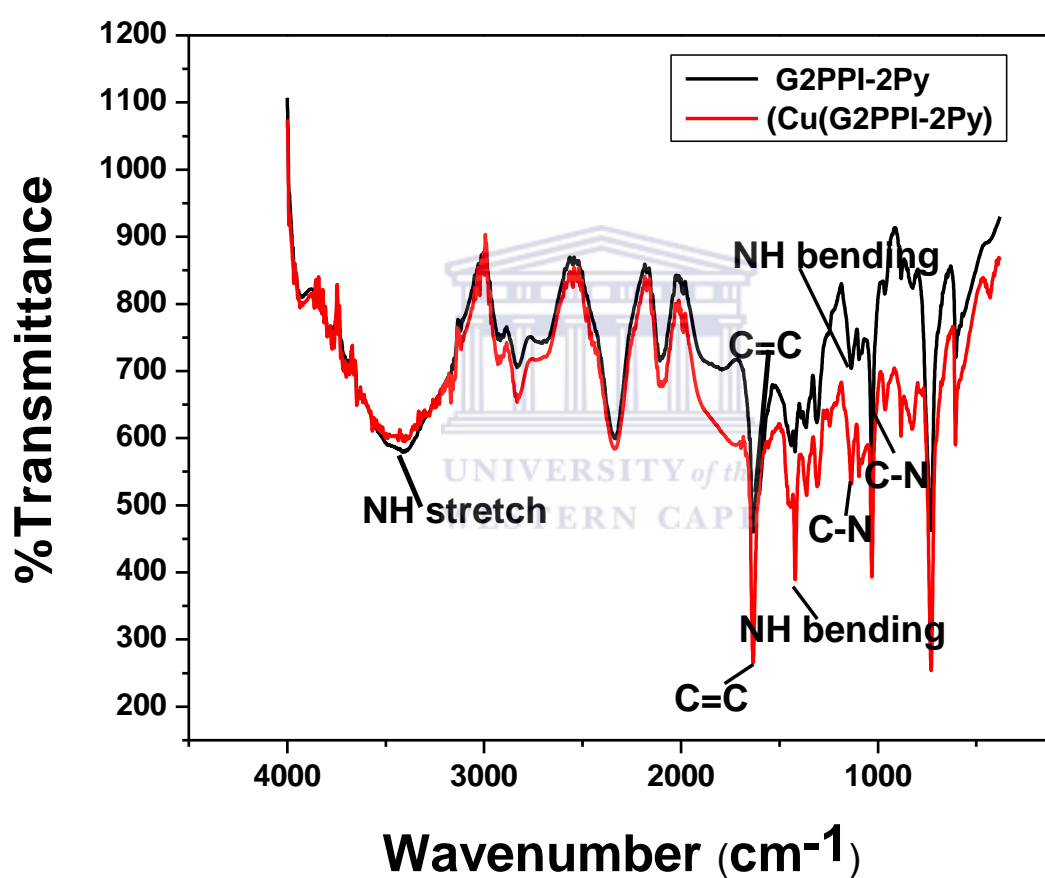
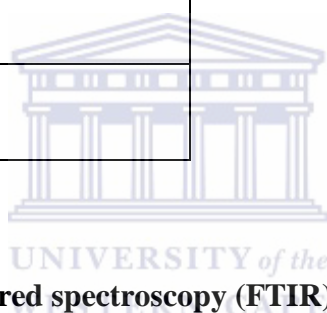


Figure 9: FTIR spectra of (Cu(G2PPI-2Py)) and G2PPI-2Py.

Table 1: Bonds and their respective frequencies in the structure of the G2PPI-2Py and (Cu(G2PPI-2Py) metallodendrimer

Frequency, cm^{-1}	Bond Type
3400-3250	N-H
1680-1640	-C=C
1335-1250	C-N Stretch aromatic
1600–1585	C-C Stretch
1250-1220	C-N Stretch aliphatic
2800-3000	CH Stretch
1640-1690	C=N



4.1.1 Fourier transformed infrared spectroscopy (FTIR)

Fourier transform infrared spectroscopy was used to determine the structure of the G2PPI-2Py dendrimer and the (Cu(G2PPI-2Py) metallodendrimer. Fig.9 shows the FTIR spectra of (Cu(G2PPI-2Py) and G2PPI-2Py while table 1 shows the types of bonds that are present in the molecules as well as their respective wave numbers. The FTIR spectra shows characteristic (NH), $\nu(\text{C}=\text{C})$, $\nu(\text{C}-\text{N})$ aliphatic bond bands at, 3413 cm^{-1} , 1642 cm^{-1} , 1306 cm^{-1} for the pyrrole ring for both the (Cu(G2PPI-2Py) and G2PPI-2Py complexes. The broad band at 3413 cm^{-1} represents the N-H stretching vibrations in the pyrrole ring while the C-N bond of the dendrimer moiety is found at 1250 cm^{-1} . The spectra of G2PPI-2Py shows out-of-plane bending of the C-H bond located at the α position in the Py ring appearing at 729 cm^{-1} while the sharp band at 1634 cm^{-1} is assigned to the N=C bond stretching vibration present in the dendrimer moiety. The appearance of these two characteristic peaks confirms the functionalization of the amine groups of PPI by 2-Py. (Cu(G2PPI-2Py) compared to G2PPI-2Py was found to have an increase in the intensities of all its peaks. This phenomenon can be attributed to the coordinative bonding that exists between the dendrimer moiety and the metal

which can sometimes be described as an artificial bond. This signifies that there was no breakage of existing bonds or formation of new bonds after addition of the copper metal. This phenomenon is also observed on the spectra of the (Cu(G2PPI-2Py) metallodendrimer where no evidence of new peaks was indicated but showing only those of covalent bonding between 2-Py and the dendrimer moiety.



4.2 Microscopic characterisation of G2PPI-2Py and (Cu(G2PPI-2Py)

4.2.1 High resolution scanning electron microscopy (HRSEM)

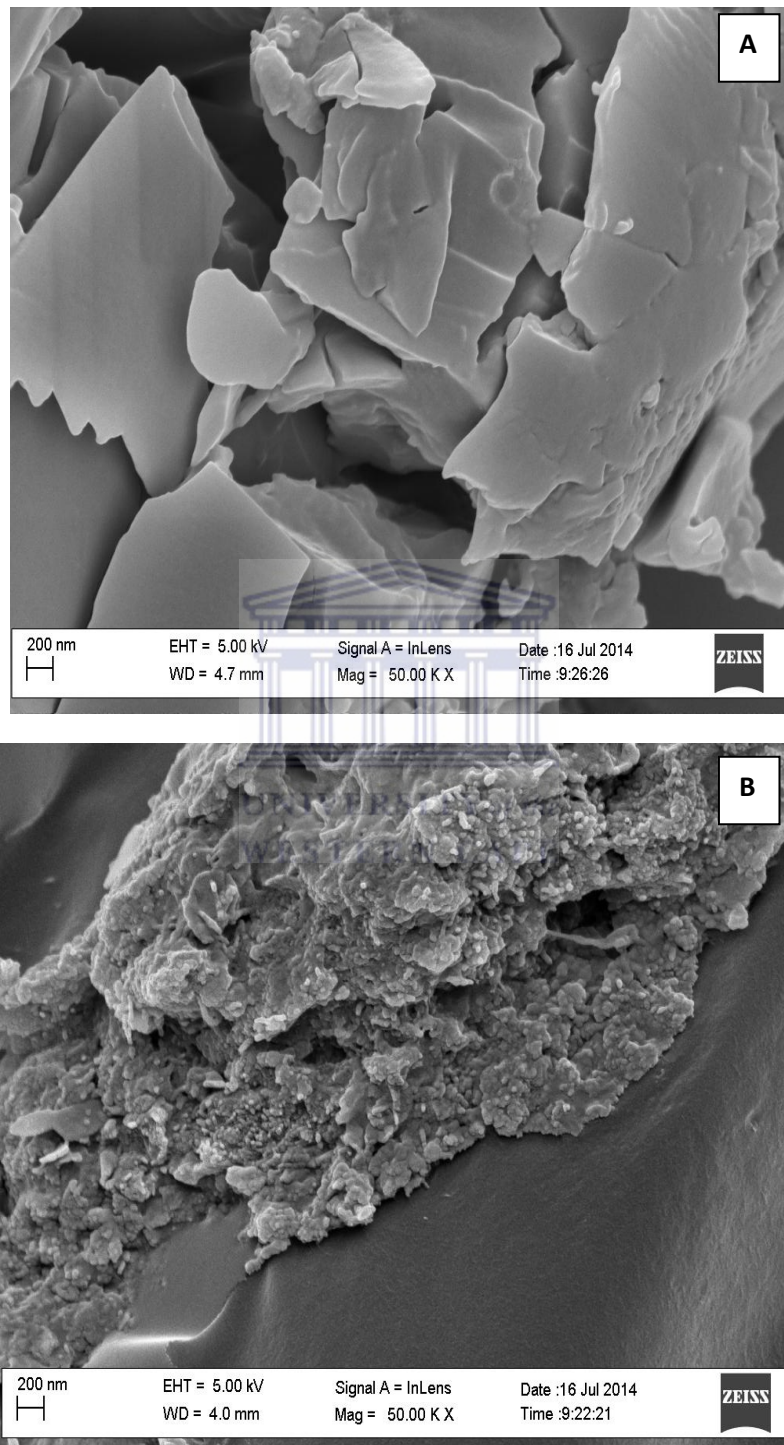


Figure 10: The High Resolution Scanning Electron Microscope (HRSEM) images of G2PPI-2Py (A) and (Cu(G2PPI-2Py) (B).

The surfaces of G2PPI-2Py Fig.10 (A) and (Cu(G2PPI-2Py) Fig.10 (B) were studied using high resolution scanning electron microscopy. The morphology of the G2PPI-2Py in Fig.10 (A) shows a rough surface and a tightly packed structure which can be attributed to the sticky nature of the dendrimer; whilst that of the (Cu(G2PPI-2Py) shows that there was a change in the surface morphology of the dendrimer moiety after it was functionalized with the copper metal. The surface became smoother and was less densely packed than the surface of the dendrimer moiety. Observed on the surface are cavities which are beneficial for entrapment or the adsorption of enzymes. These cavities allow for much more enhanced stability of the enzyme onto the electrode thus act as good support material for their application in biosensor development.



4.2.2 High resolution transmission Electron Microscope (HRTEM)

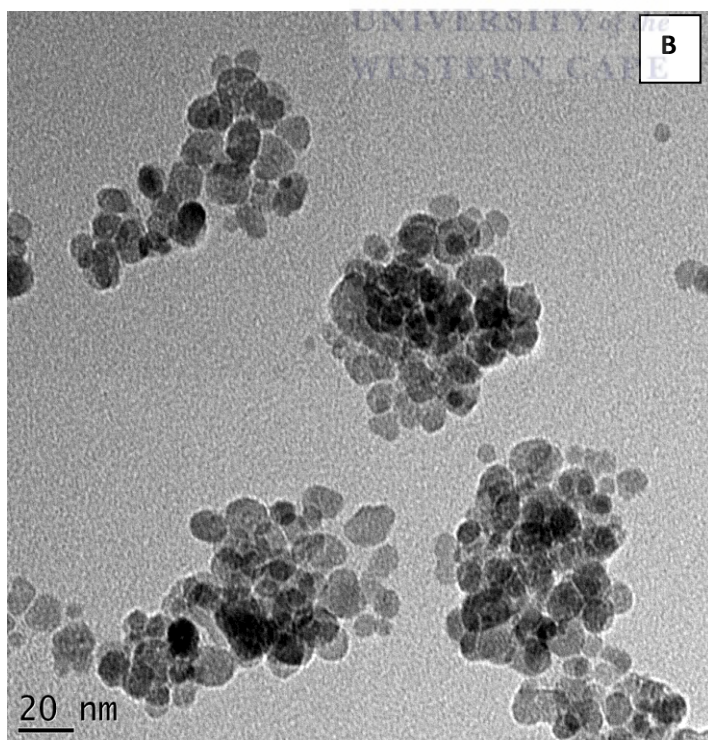
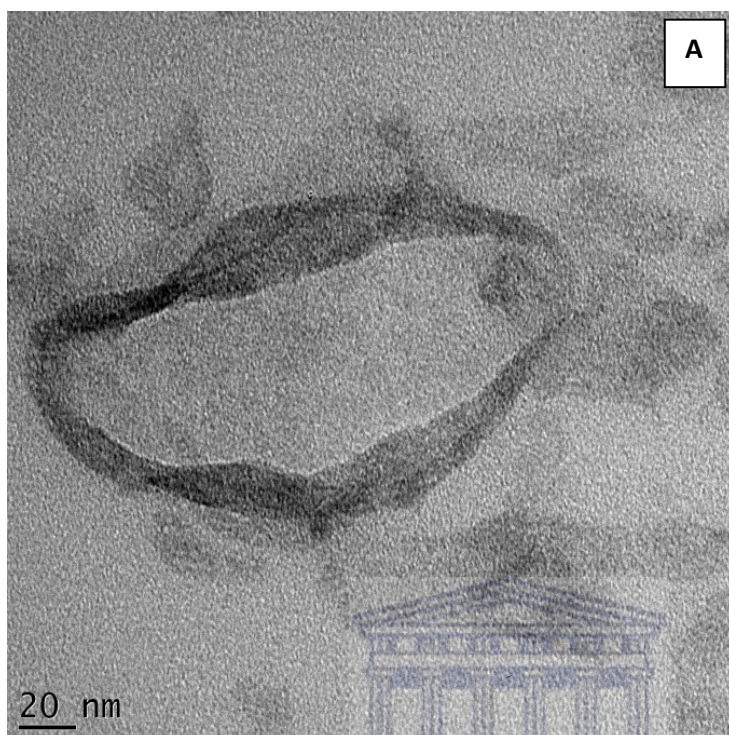


Figure 11: The High Resolution Transmission Electron Microscope (HRTEM) images of G2PPI-2Py (A) and (Cu(G2PPI-2Py) (B)

HRTEM determines the shape and size of nanoparticles. In this study it was used to determine the size and shape of copper nanoparticles present in the (Cu(G2PPI-2Py) complex. Fig.11 (A) and (B) represent the internal structures of the G2PPI-2Py and (Cu(G2PPI-2Py) components respectively. The structure of G2PPI-2Py shows the spherical shape of the dendrimer which is the typical shape of dendrimers. The observed copper nanoparticles in Fig.11 (B) are agglomerated due to their small size and their high surface area. The particles are seen to have formed adjacent bond with other nanoparticles due to their smaller size, higher relative surface area, and higher relative numbers of surface atoms. This phenomenon resulted in their atoms having unsaturated coordinations further resulting in the atom having vacant coordination sites thus forming more bonds by bonding with other atoms. The particles were found to be in the range of 15-20 nm with an average particle size of 17 nm.



4.2.3 Energy dispersive spectroscopy (EDS)

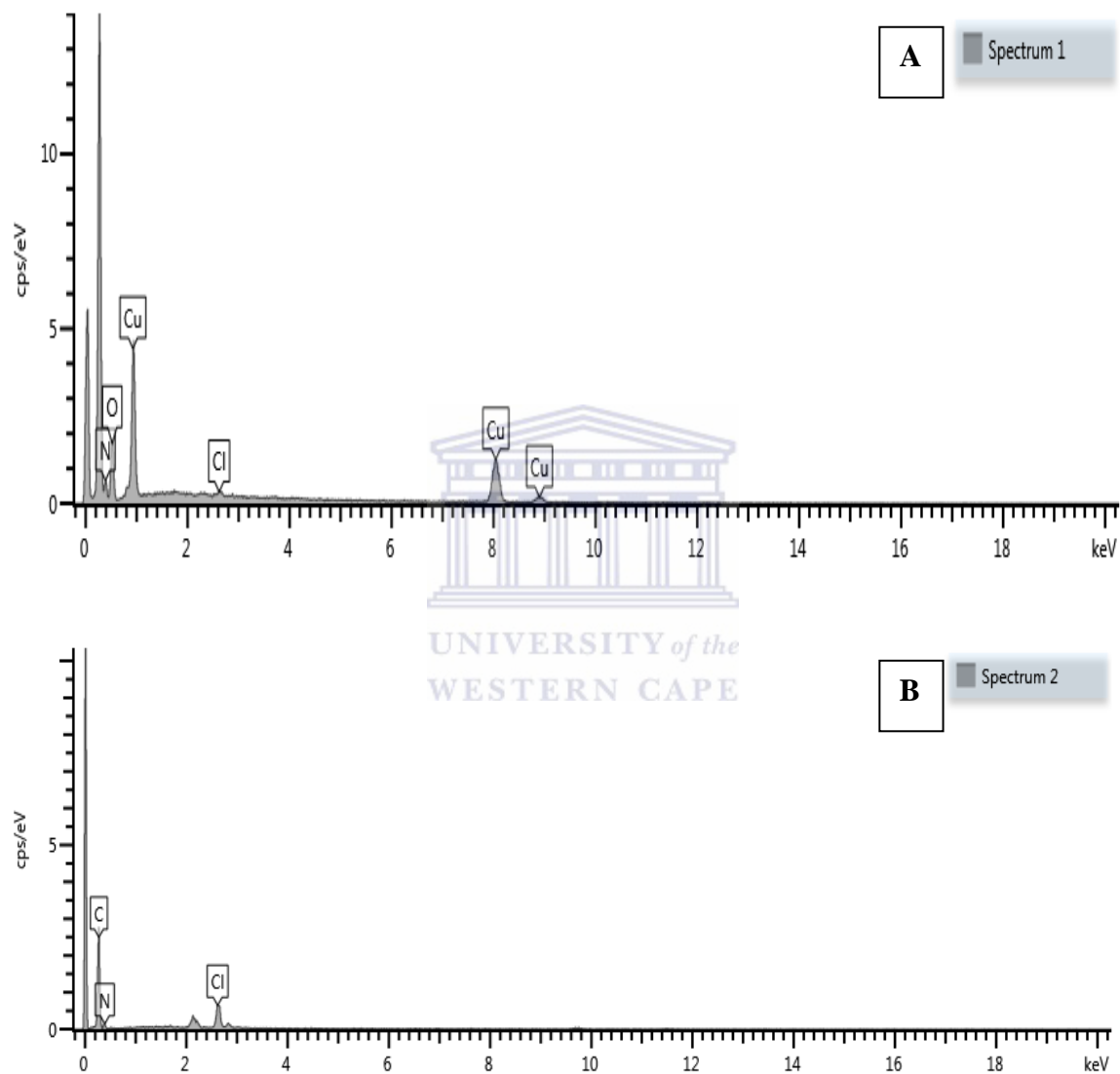


Figure 12: The Energy Dispersive X-ray radiation (EDX) Spectrum of the (Cu(G2PPI-2Py) (A) and (B) G2PPI-2Py.

Energy Dispersive X-ray radiation (EDX) was used to determine which elements were present in G2PPI-2Py (Fig.12 (B)) and (Cu(G2PPI-2Py) (Fig.12(A)) metallodendrimer. The

EDX spectra of G2PPI-2Py indicates that the material showed the presence of nitrogen and carbon atoms. On Fig. 12(A) it was observed that there was presence of copper which was the main metal of interest as its presence means there was successful functionalization of the copper into the G2PPI-2Py dendrimer. The presence of nitrogen in this spectrum is in line with the structure of the dendrimer which consists of nitrogen atoms. The oxygen is due to the unreacted oxygen from the copper acetate which was used as the source of the copper metal thus; it can be regarded as an impurity. The EDS of the dendrimer indicated the elements carbon, nitrogen and chlorine with chlorine being an impurity that was present in the compound. Carbon and the nitrogen were expected as the structure of G2PPI-2Py contains nitrogen and carbon atoms only.

4.3 Electrochemical polymerization characterisation of PPy and (Cu(G2PPI)-co-PPy)

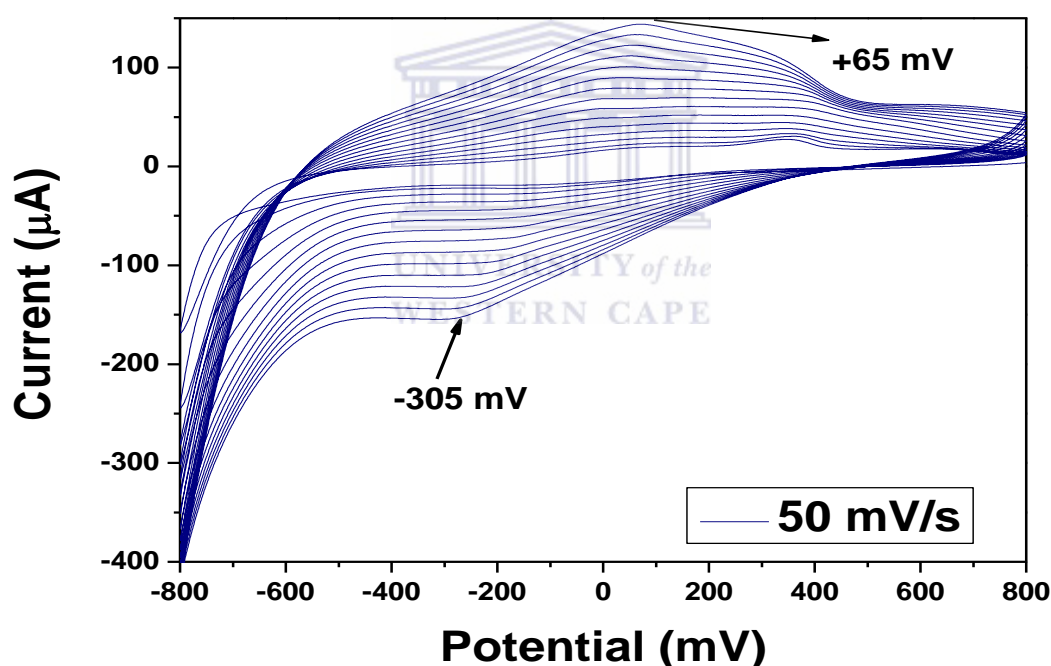


Figure 13: Electrochemical polymerization of Py onto Pt electrode in 0.1 M lithium perchlorate (+800 mV) to (-800 mV) at scan rate 50 mV/s.

Fig.13 shows cyclic voltammograms for the electrochemical polymerization (+800 mV to -800mV) of pyrrole on a Pt electrode performed at a scan rate of 50 mV/s for 30 cycles in lithium perchlorate. At the initial oxidation step, the radical cation of the monomer is formed and reacts with other monomers present in solution to form oligomeric products and then the polymer. It is observed that there is an increase in current with increasing number of cycles,

implying deposition of an electroactive material on the surface of the electrode. Polymerisation of the monomer shows a reduction peak at -305 mV which is due to the monomer being deposited on the electrode surface. While the peak at +65 mV is due to the formation of polymer chains. There is an observable shift in the anodic potential towards the negative potential with an increase in number of cycles. This is due to the extended conjugation in the polymer which results in a lowering of the oxidation potential compared to the monomer. The polymer is therefore more easily oxidized at the applied potential which is the oxidation potential of the monomer. Therefore, the synthesis and doping of the polymer are generally done simultaneously. The anion is incorporated into the polymer to ensure the electrical neutrality of the film and at the end of the reaction, a polymeric film of controllable thickness is formed at the anode.

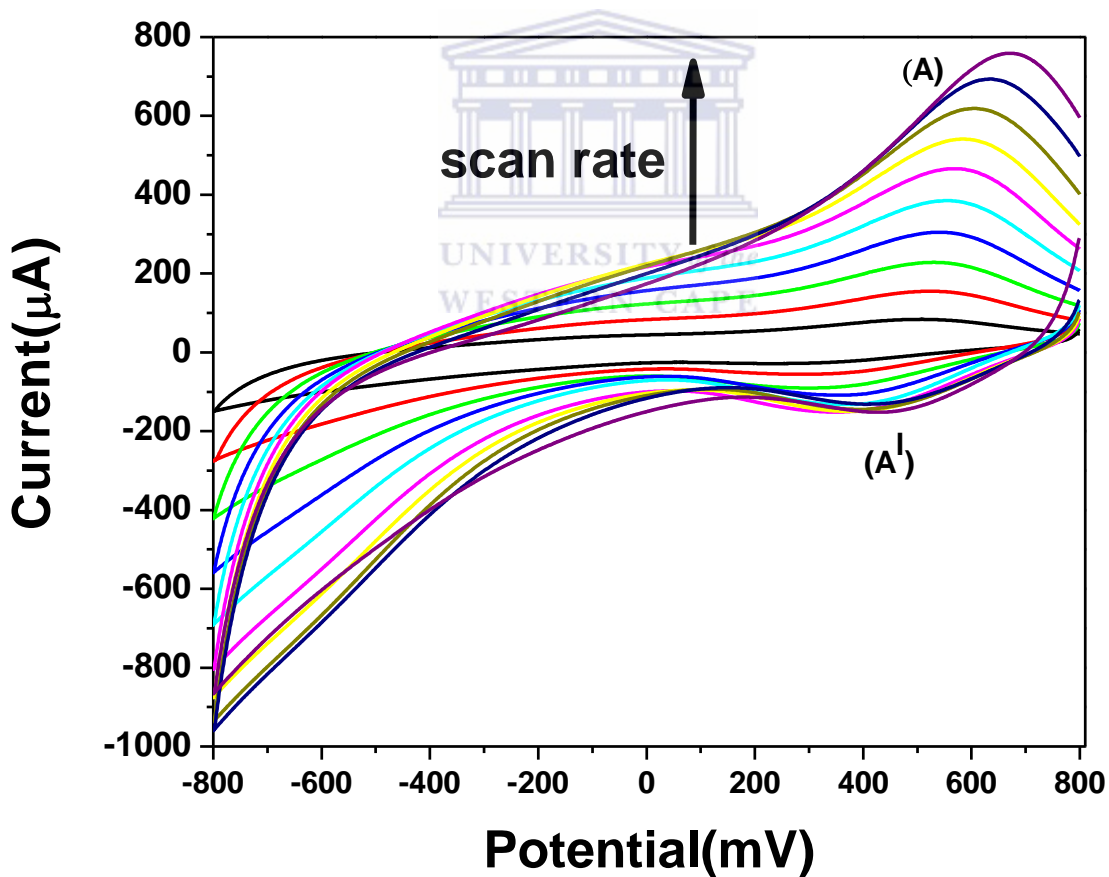


Figure 14: Cyclic voltammogram of PPy/Pt electrode in 0.1 M pH 7.4 phosphate buffer at scan rates (10 mV/s to 100 mV/s).

Fig.14 represents the cyclic voltammogram of Py/Pt in 0.1 M pH 7.4 phosphate buffer at the potential window of (+800 mV to -800 mV). There are two peaks that are observable in the voltammograms A and A¹ where the anodic peak (A) at +550 mV is due to the oxidation of the pyrrole while the cathodic peak (A¹) at +495 mV is due to the deposited pyrrole onto the electrode surface. There is a shift of the anodic potential towards more positive potential with an increase in scan rate from +550 to +620 mV showing a more readily oxidised species. There is an observable linear increase in the anodic peak current with an increase in scan rate (as shown in Fig.14) which indicates the occurrence of the electrochemistry of surface confined species. There is no shift in the cathodic peak current indicative of a surface bound species. ΔE_p [$E_{p,a} - E_{p,c}$] was calculated for the polymer film grown at different scan rates resulted in a value of ΔE_p greater than 65 mV.

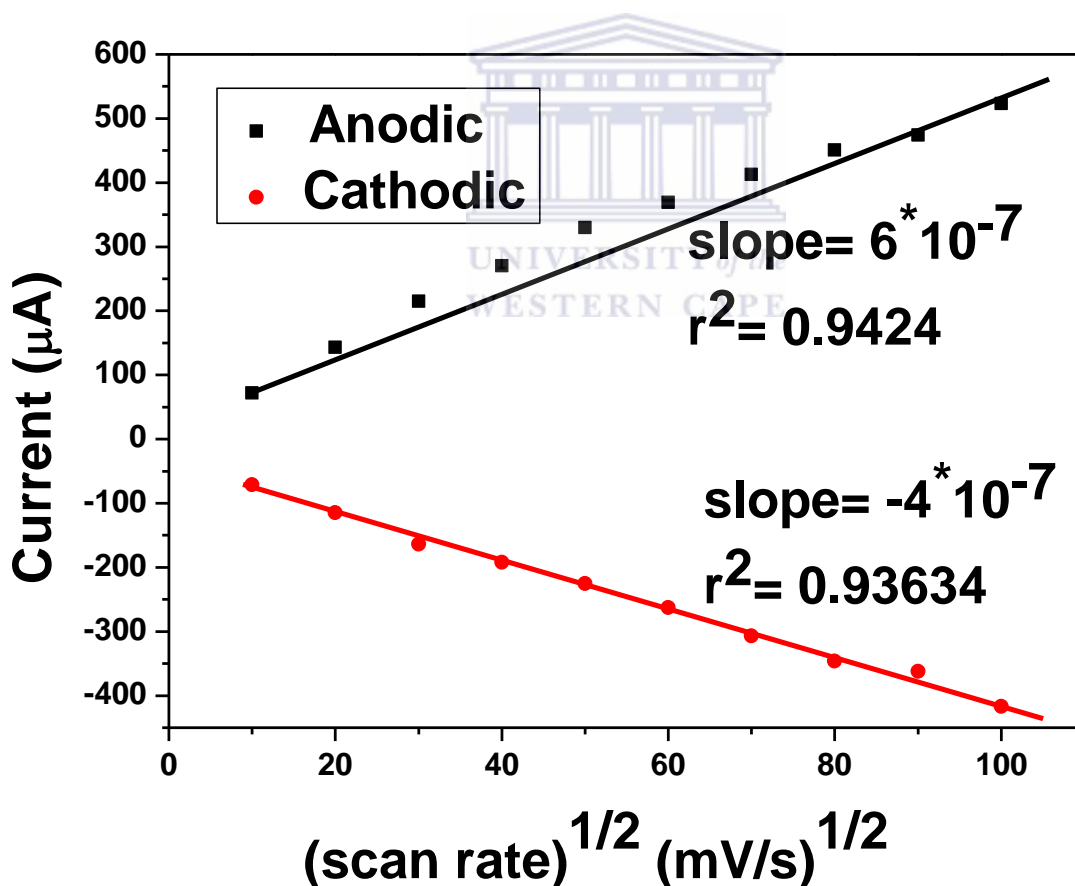


Figure 15: Randle Sevcik plot of PPy in 0.1M phosphate buffer PH 7.4 at different scan rates for the determination of the diffusion co-efficient.

Fig.15 shows the linear dependency of the current on the scan rate of the redox couple A/A¹ shown in Fig. 14. This is indicative of a thin surface bound conducting electro-active polymer film undergoing a rapid reversible electron transfer reaction along the polymer backbone possibly through the pyrrole ring units making up the chain of the polymer. The surface concentration of the polymer was estimated to be 1.00x 10⁻⁴ mol/cm⁻³ (0.6 ± 0.1) using the Brown-Anson method illustrated as follows:

$$I_p = \frac{n^2 F^2 \Gamma^*_{(PPy)} A v}{4RT} \quad (1)$$

where n represents the number of electrons involved in the reaction, F is the Faradays constant (96,584 C/mol), $\Gamma^*_{(PPy)}$ is the surface concentration of the PPy film (mol/cm²), v is the scan rate (mV/s), A is the electrode area of the electrode (0.0201 cm²), R is the universal gas constant (8.314 J/(mol K)) and T is the temperature of the system (298 K). The magnitude of the peak currents was seen to increase upon increment of the scan rate suggesting that the peak currents are diffusion controlled.

Randle Sevčik Plot given, for analysis of diffusion controlled reactions:

$$i_p = 0.0463nFA \left[\frac{nF}{RT} \right] C_0^* D_0^{1/2} v^{1/2} \quad (2)$$

Where I_p = (Peak Current in μ A), n = 1 (number of electrons), F = 96485 C/mol (Faradays Constant), A = 0.0201 cm² (area of the electrode), C_0^* = 1.00x 10⁻⁴ mol/dm² (Concentration of bulk substrate concentration), R = 8.314 J mol/ K (Gas Constant), T = 298.15 K (absolute Temperature) and v = (Scan Rate in V/s) and D_0 (diffusion co-efficient).

D_0 is the electron charge transport coefficient sometimes also known as the rate of electron charge propagation along the polymer chain. Fig.14 indicates an oxidation reaction that was occurring at E_{pa} which was seen to be diffusion controlled with a correlation co-efficient of $R^2 = 0.9424$ and a diffusion co-efficient of $D_0 = 1.243 \times 10^{-5}$ cm²/s; indicating a faster electron transfer kinetics within the diffusion layer. The reduction current peak (E_{pc}) had a correlation co-efficient of $R^2 = 0.9634$ linearity in the Randle Sevčik plots obvious case was that this reductive reaction that was occurring at that potential was diffusion controlled, and a

diffusion co-efficient of $5.528 \times 10^{-5} \text{ cm}^2/\text{s}$ indicating a slower electron transfer compared to the anodic electron transfer.

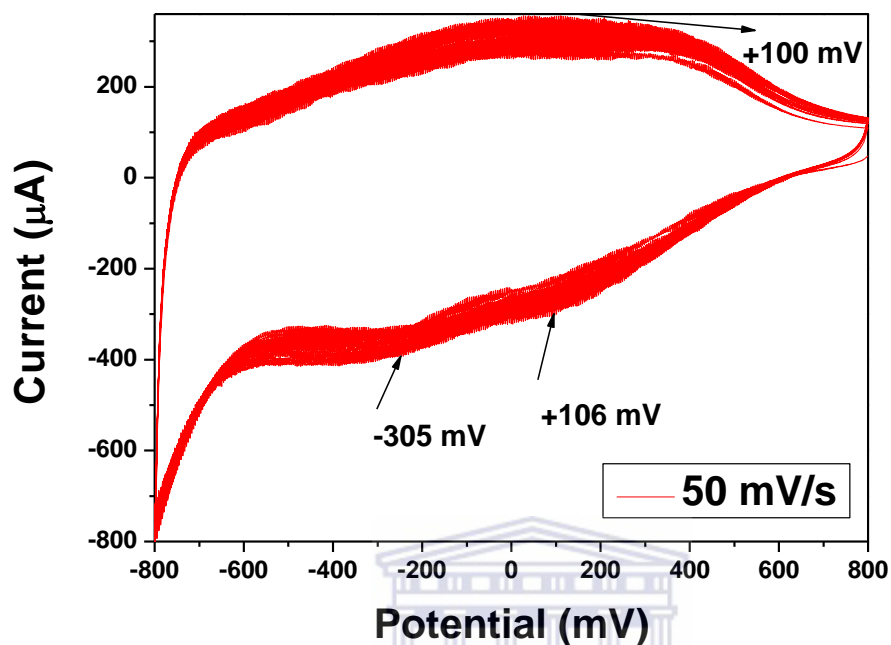


Figure 16: Electropolymerization of Py onto Cu-PPI-2py/Pt electrode in 0.1 M lithium perchlorate at 50mV/s.

Fig.16 shows the cyclic voltammograms for the electrochemical polymerization (at the potential window of +800 mV to -800mV) of pyrrole on Pt electrode performed at a scan rate of 50 mV/s for 30 cycles in lithium perchlorate. The electrochemical polymerisation of pyrrole is characterised by an increase in current with an increase in the number of cycles. There is observed separation between the anodic and cathodic scans which are attributed to the good conductivity of the star copolymer doped with copper nanoparticles. The broadness of the cathodic and anodic peaks is due to the slow movement of the electrons during the polymerisation process. The cathodic peak at -305 mV is due to the dendrimer attached on the surface of the electrode and peak at +106 mV can be attributed to the deposition of pyrrole onto already existing copper metallodendrimer on the surface of the electrode, while the peak at +100 mV in the anodic scan can be attributed to the formation of the copolymer chain.

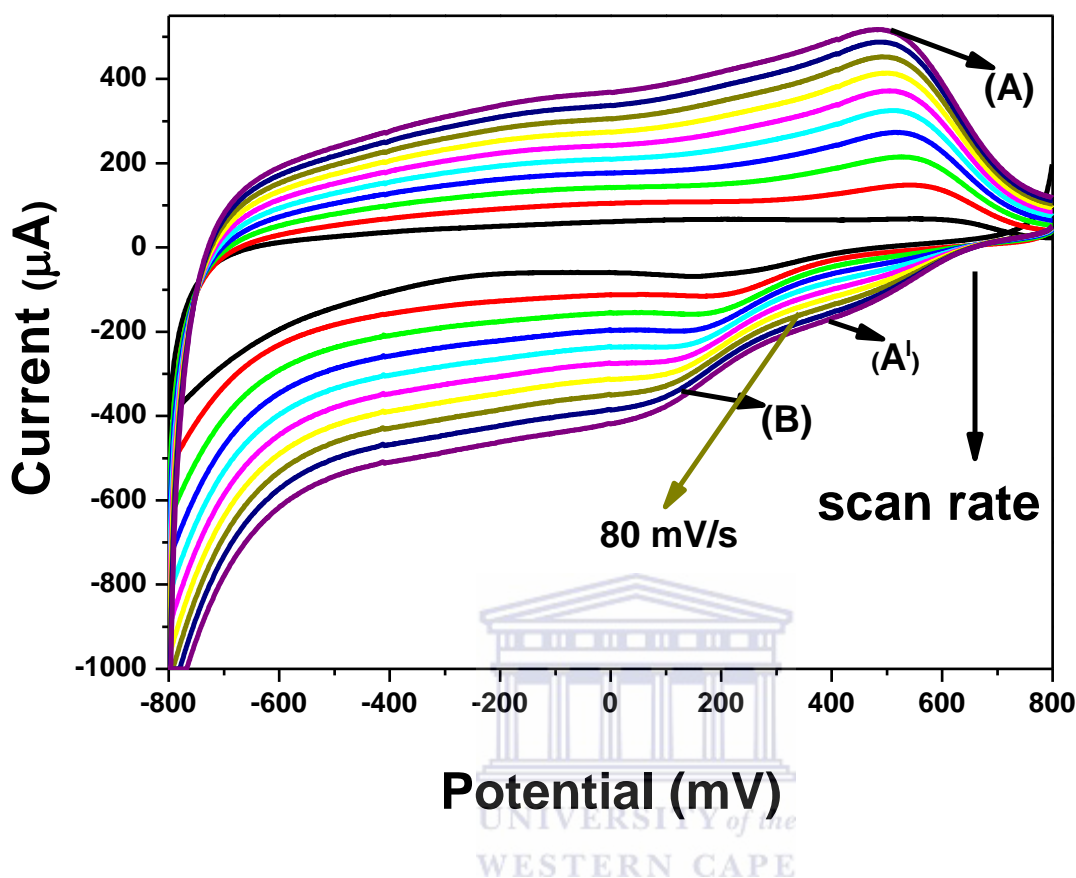


Figure 17: Cyclic voltammogram of (Cu(G2PPI)-co-PPy)/Pt in 0.1 M phosphate buffer pH 7.4 at the potential window of +800 mV to -800 mV.

Fig.17 shows the cyclic voltammogram of Cu(G2PPI)-co-PPy, where 3 faintly observable peaks are denoted by A, A¹ and B. The oxidation state of copper in the complex was found to be +2 and the number of electrons that are found in the system were determined to be n=1. $\Delta E_p [E_{p,a} - E_{p,c}]$ was calculated for the polymer film grown at different scan rates resulted in a value of ΔE_p lower than 65 mV as shown in table 2. This suggested that the polymer exhibited reversible and a fast electrochemistry. The cathodic peak at +146.36 mV denoted by (B) is seen to be increasing with an increase in scan rate. There is an observable cathodic shift in the peak potential to +55.79 mV due to the extended conjugation in the polymer which results in the lowering of the oxidation potential of the polymer. The anodic peak (+484.86 mV) denoted by (A) is due to the change in the oxidation state of the copper metal that is present in the copper complex as seen with the mechanism $\text{Cu}^+ \leftrightarrow \text{Cu}^{2+} + e^-$. There is

no shift in the peak with an increase in scan rate, this is indicative of a surface bound species thus the (Cu(G2PPI)-co-PPy)copolymer is a surface bound species. There is an increase in the anodic peak currents of the (Cu(G2PPI)-co-PPy) which is indicative of the conductivity of the material. The cathodic peak (+435 mV) signified by (A¹) is given by the mechanism $\text{Cu}^{2+} + \text{e}^- \leftrightarrow \text{Cu}^+$. There was an increase in the cathodic current with an increase in scan rate. There was a slight increase in the cathodic peak and a broadening of the peak resulting in the plateau and disappearance of the peak at the scan rate of 80mV/s signifying a slow movement of the electron in the system. In Fig.18 it is indicated that the oxidation reaction occurring at E_{pa} was diffusion controlled with correlation co-efficient of $r^2 = 0.9111$ with a diffusion co-efficient which was found to be $D_0 = 8.6374 \times 10^{-5} \text{ cm}^2/\text{s}$; indicating a slower electron transfer kinetics within diffusion layer. However, the reduction current peak E_{pc} had a correlation co-efficient of $r^2 = 0.8976$ indicating no linearity in the Randle Sevčik plot as a result of the fact that the reductive reaction occurring at that potential was adsorption controlled rather than diffusion controlled, with a determined diffusion co-efficient of $5.5270 \times 10^{-5} \text{ cm}^2/\text{s}$.

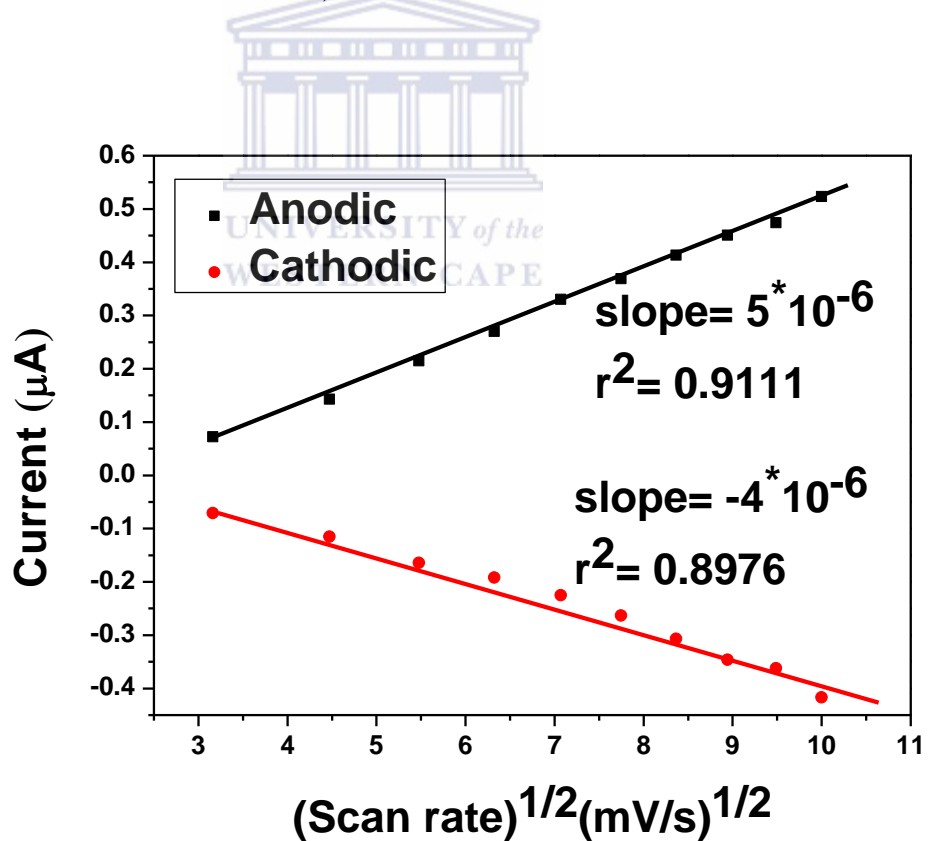


Figure 18: Randle Sevčik plots of (Cu(G2PPI)-co-PPy)/Pt at different scan rates studied in 0.1 M PBS, pH 7.4 for determination of the diffusion co-efficient D_0 .

Table 2: Electrochemical studies of PPy and (Cu(G2PPI)-co-PPy)

Polymer	E_{pa} (mV)	E_{pc} (mV)	E⁰ (mV)	ΔE_p = E_{pc} - E_{pa} (mV)	n = 60/ΔE_p	I_{pa}/I_{pc}
PPy	41.286	-24.156	83.35	90	1	2
Cu(G2PPI)-co-PPy	54.029	-36.02	90.04	60	2	2
Cu(G2PPI)	54.00	-37.10	89.05	91	1	2



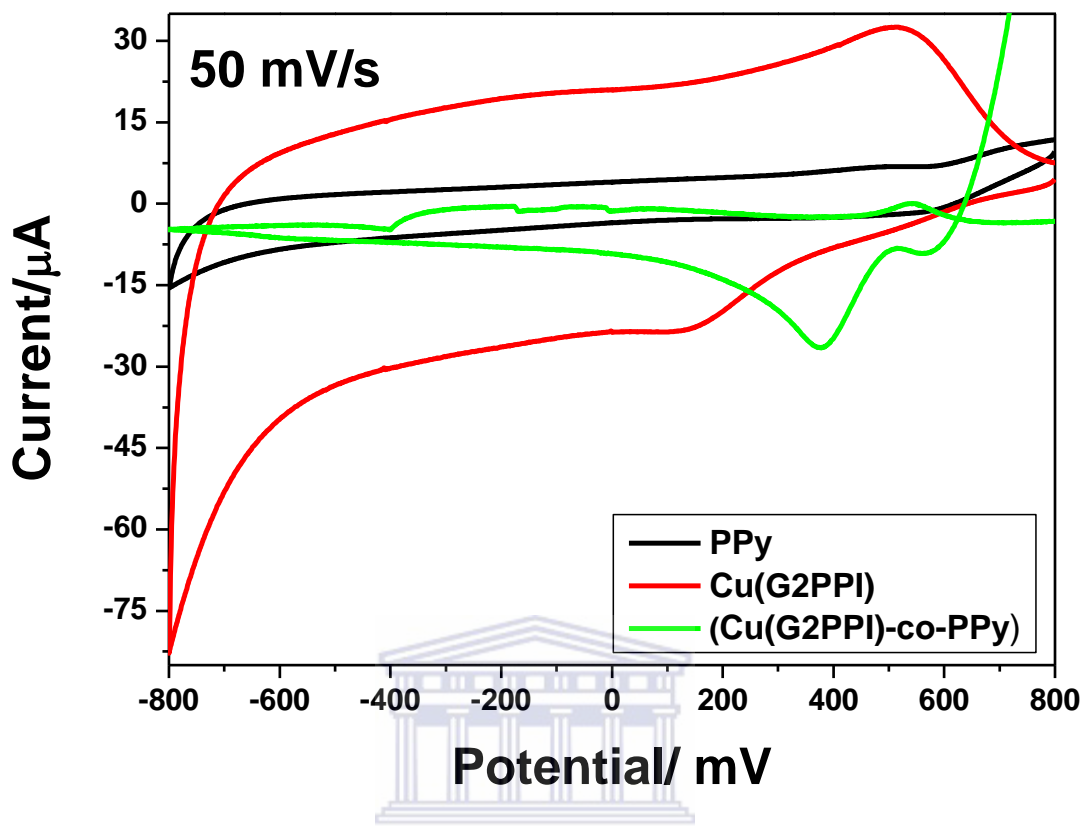
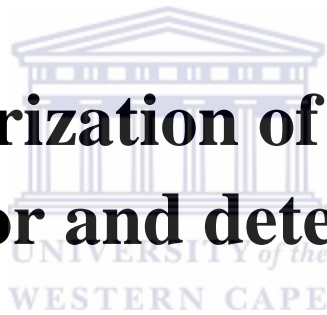


Figure 19: Cyclic voltammogram of PPy//Pt, Cu(G2PPI) and Cu(G2PPI)-co-PPy//Pt in 0.1M phosphate buffer pH 7.4 at 50 mV/s.

Comparative studies between PPy and (Cu(G2PPI)-co-PPy) represented by Fig.19 show that there is an observed increase in the formal potential (E^0) for the (Cu(G2PPI)-co-PPy) system than the PPy system as illustrated in table 2, where (E^0) was 90.04 mV, 89.05 mV and 83.35 mV for (Cu(G2PPI)-co-PPy), Cu(G2PPI) and PPy respectively. There is also an increase in the observed peak current indicating that (Cu(G2PPI)-co-PPy) has better current resolution and thus is more conductive than PPy and Cu(G2PPI). This confirms that this co-polymer is a more suitable material for application in the construction of biosensors since it will function as a better electron mediator than Cu(G2PPI) and PPy alone.

Chapter 5

Characterization of CYP 3A4 nanobiosensor and detection of DLV



5.0 Summary

This chapter deals with characterisation of the CYP 3A4/Pt and CYP 3A4/(Cu(G2PPI)-co-PPy)/Pt and their response measurements using CV.

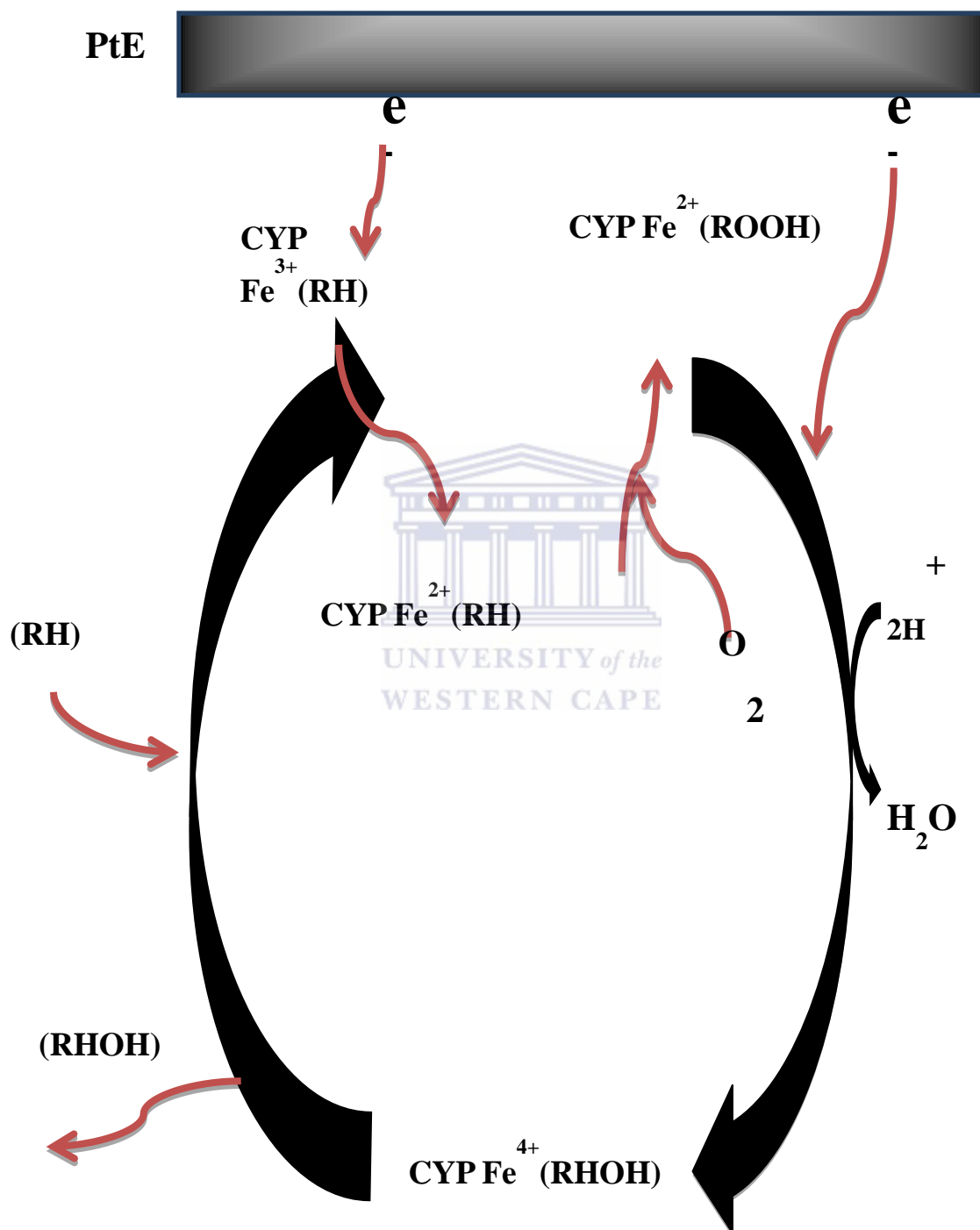


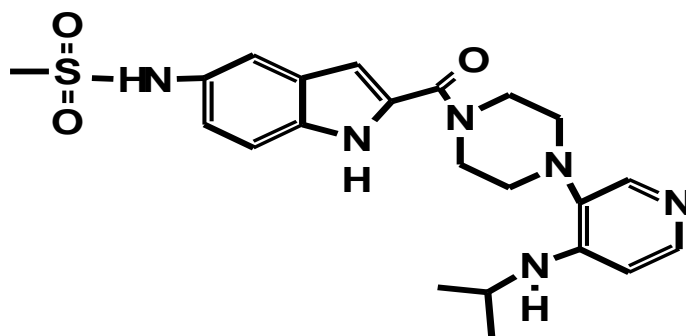
Figure 20: Reaction scheme showing the metabolism of delavirdine using the CYP 3A4/(Cu(G2PPI)-co-PPy)/Pt nanobiosensor.

KEY:

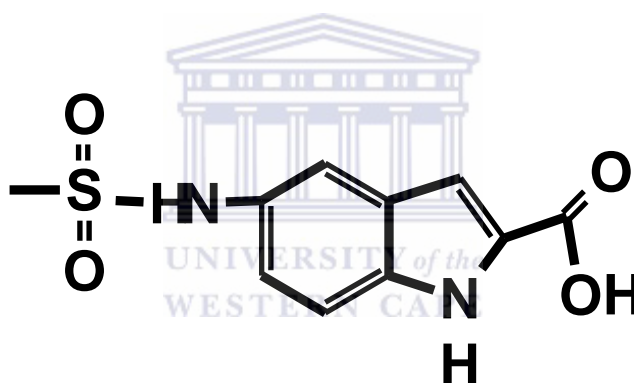
CYP^{4+, 3+, 2+} - Different oxidation states of Cytochrome P450-3A4

ROOH – delavirdine

ROO-H – indole carboxylic acid



Delavirdine (A)



Indole carboxylic acid (B)

Figure 20(A) and (B) represents the structures of delavirdine and indole carboxylic acid respectively.

Fig.20 describes the binding of delavirdine drug onto the active site of the enzyme followed by the one electron electrochemical reduction of the hexa-coordinated low-spin ferric enzyme (Fe³⁺) to the high spin ferrous enzyme (Fe²⁺). This form of the enzyme has a high affinity for oxygen and thus binds molecular oxygen present in the solution onto the active site resulting in another electron reduction and formation of by-product. From the scheme in Fig.20 the compounds RH and ROH are Delavirdine and Indole carboxylic acid respectively.

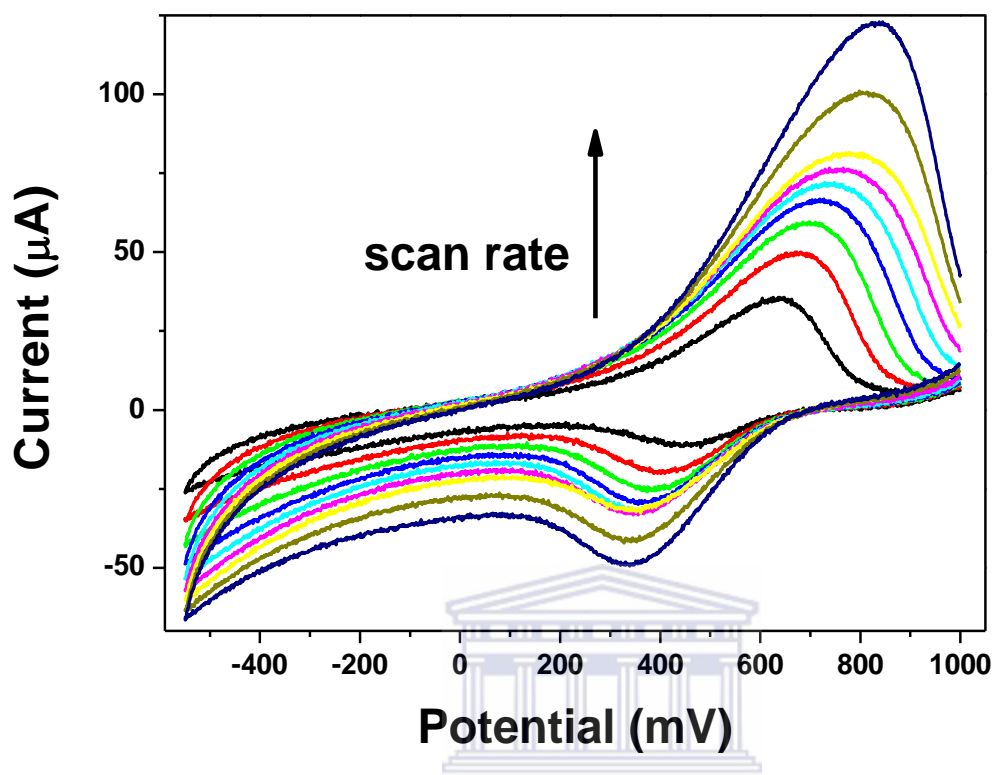


Figure 21: Cyclic voltammogram of the nanobiosensor at different scan rates (10, 20, 30, 40, 50, 60, 70, 80 and 90 mV/s) in 0.1 M PBS pH 7.4.

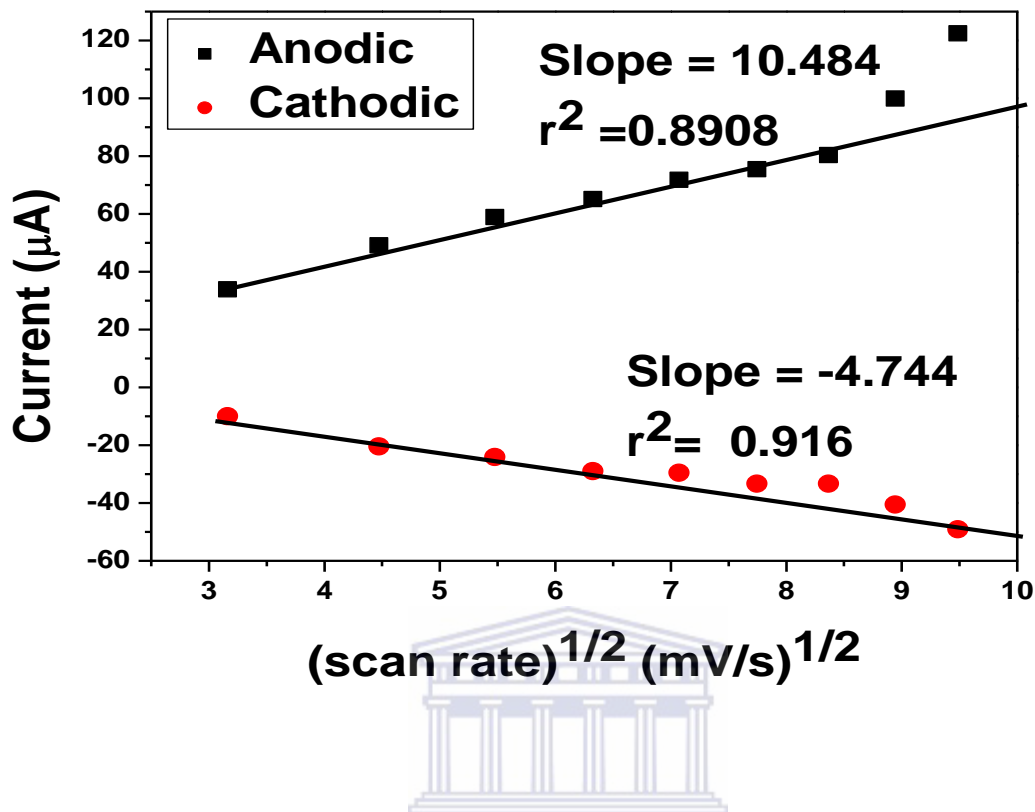


Figure 22: Randle Sevcik plot of CYP 3A4/(Cu(G2PPI)-co-PPy)/Pt biosensor in 0.1M PBS pH 7.4 at different scan rates for the determination of the diffusion co-efficient.

The voltammogram in Fig.21 shows an increase in current with an increase in scan rate. At lower scan rates (10 - 50mV/s) there is a linear increase in the current with an increase in scan rate. At scan rates from (60 - 90) mV/s there is a sharp increase in the current which is indicative of the instability in the nanobiosensor. In this context it is an indication of electron fouling thus the use of scan rates below 20 mV/s would be favourable for the studies using this nanobiosensor system to avoid such instance. Observed is a shift in the anodic potentials towards more oxidative potentials characteristic of a species which is more prone to oxidation. The peaks were characterised by the reduction peak at $E_{pc} = +403$ mV is deduced to be due to the catalytic current produced by the nanobiosensor due to the presence of the enzyme. The Randle Sevcik plot (Fig.22) show the linear dependency of the current on the scan rate. It indicated that the reduction reaction that was occurring at $E_p = +403$ mV was diffusion controlled with correlation co-efficient of $r^2 = 0.916$ and the diffusion co-efficient was found to be $D_0 = 6.917 \times 10^{-5} \text{ cm}^2/\text{s}$, indicating a faster electron transfer kinetics within the diffusion layer of the nanobiosensor. However the oxidation peak current occurring at E_{pa}

= +200 mV had a correlation co-efficient of $r^2 = 0.8908$ indicating no linearity in the Randle Sevčík plots an adsorption controlled process is assumed, as opposed to diffusion controlled.

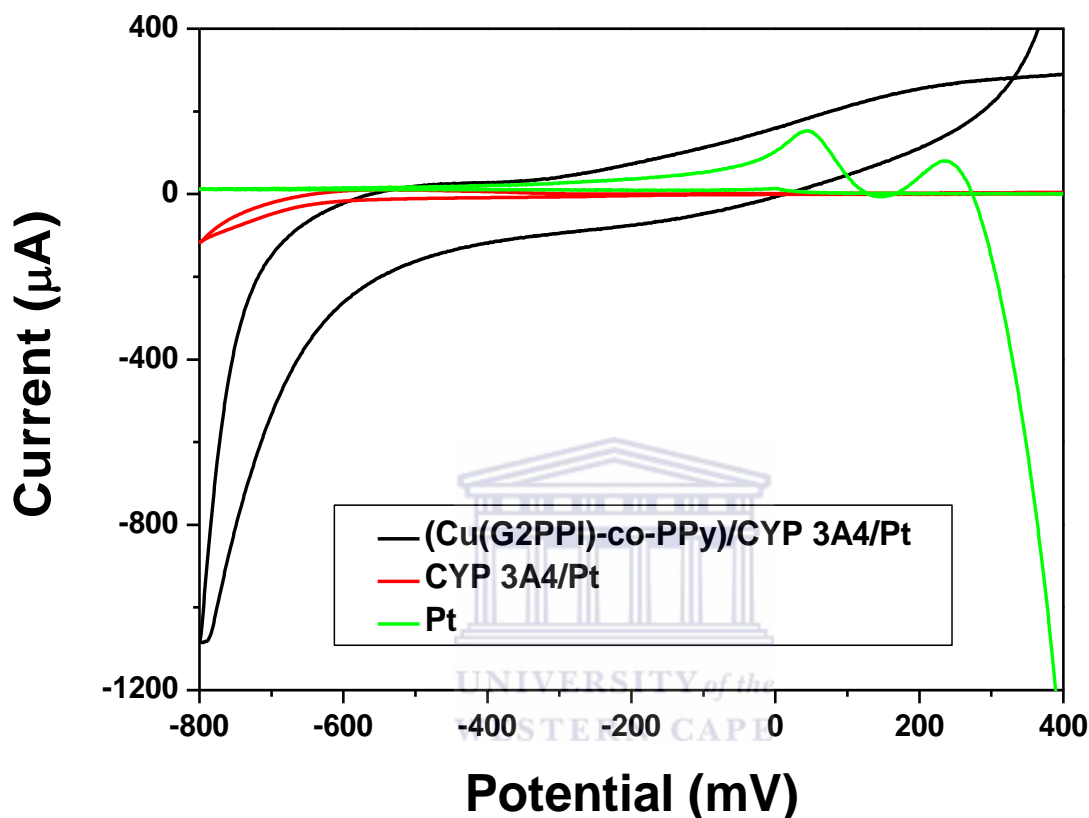


Figure 23: Cyclic voltammograms of the Pt electrode, CYP3A4/PtE and CYP3A4/(Cu(G2PPI)-co-PPy)/PtE nanobiosensor in PBS pH 7.4.

Fig.23 shows cyclic voltammograms of Pt electrode, CYP3A4/PtE and CYP3A4/(Cu(G2PPI)-co-PPy)/PtE modified onto platinum electrode in the absence of the analyte. There is a low peak current observed on the CYP 3A4/PtE biosensor and an increase in the peak current on the CYP3A4/(Cu(G2PPI)-co-PPy)/PtE nanobiosensor which is indicative of the conductivity and catalytic activity of the (Cu(G2PPI)-co-PPy) which facilitates the transfer of electrons. Although a catalytic reaction or the electron transfer reaction is possible between the enzyme and the electro active material within the bulk of the solution, this reaction will occur at a distance to the electrode surface. This is due to the fact that the stability of enzyme molecule onto the electrode surface is not good enough to hold

the enzyme in-close proximity to the electrode surface. Thus one would expect low electrochemical reactions, slow enough not to even be observed.

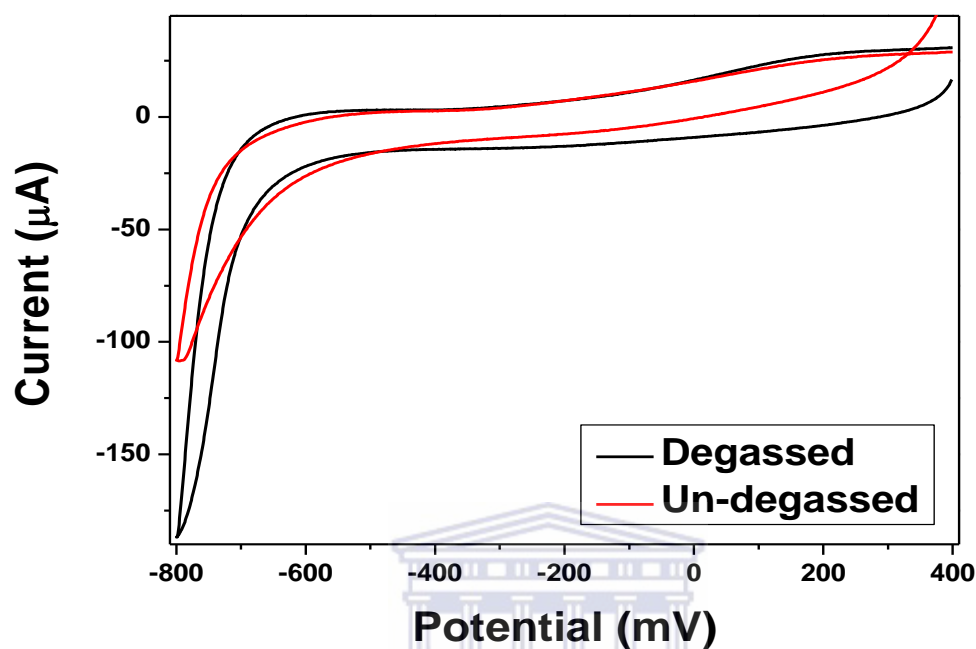


Figure 24: Cyclic voltammograms of the CYP 3A4/(Cu(G2PPI)-co-PPy)/Pt under aerobic and anaerobic conditions in 0.1M PBS PH 7.4 at scan rate 10 mV/s.

The cyclic voltammograms represented in Fig.24 were obtained in the absence of the drug were performed in anaerobic and aerobic solutions. In the presence of oxygen, the nanobiosensor showed an increase in the cathodic and anodic peak current with an onset potential of -160 mV (vs Ag/AgCl) which is indicative of the oxygenation of CYP 3A4 heme Fe atom being coupled to the electron transfer reaction that occurs in argon degassed medium.

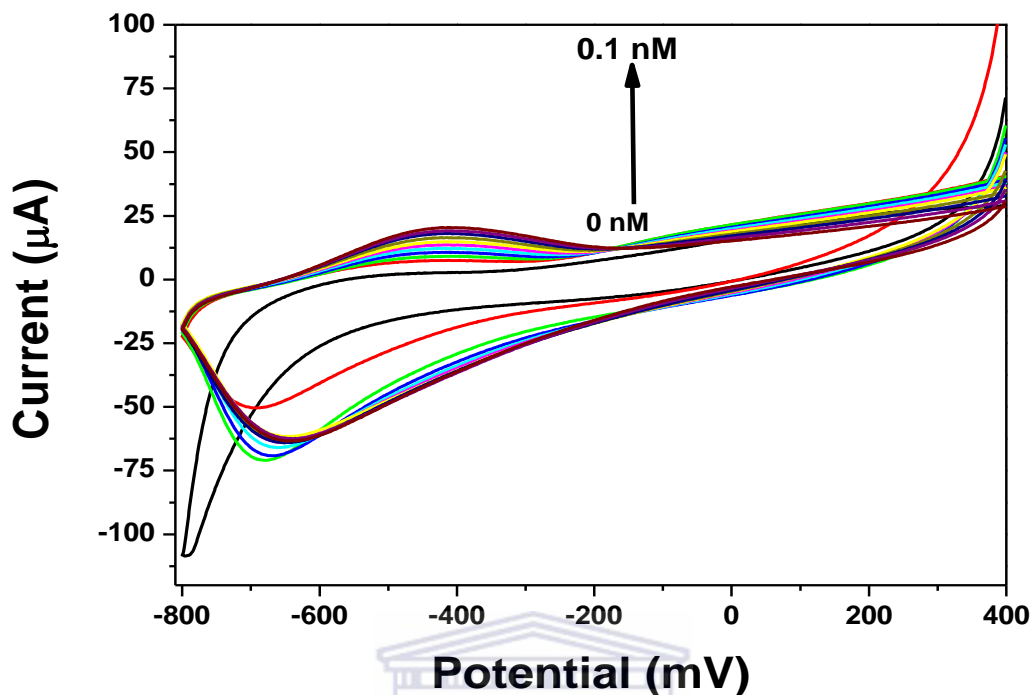


Figure 25: Cyclic voltammogram of the CYP3A4/(Cu(G2PPI)-co-PPy)/Pt nanobiosensor response of DLV drug in 0.1M PBS pH 7.4.

The electrochemical behaviour of the nanobiosensor was evaluated using CV. CV was used to study the behaviour of the nanobiosensor to successive additions of delavirdine drug under aerobic conditions as shown in Fig.25. The presence of oxygen in the system is essential for the binding of oxygen to the heme group that is present in the CYP3A4 enzyme in the Fe^{2+} state. In the absence of the analyte there is no oxidation and reduction peaks observed. With successive addition of the delavirdine drug there was an observed increase in the peak currents resulting from the current response generated by the electron transfer reaction occurring between the enzyme CYP3A4 immobilised and the substrate delavirdine. There was a slight shift in the potential towards positive potential values with an increase in substrate concentration which can be attributed to the conversion of Fe^{4+} oxidation state of the CYP 3A4 enzyme to Fe^{3+} which can be attributed to the reduction of the CYP3A4 enzyme by delavirdine. From the analyte concentration of 0.1 nM there was no observable change in the peak current which can be attributed to the saturation of the biosensor system where the analyte can no longer be bound on to the active site of the CYP 3A4.

From the linear range calibration curve for the CYP 3A4 detection plot as seen in Fig.25 the limit of detection and sensitivity of the nanobiosensor towards delavirdine were estimated and calculated to be 0.025 nM and 0.379 $\mu\text{A}/\text{nM}$. The biosensor has a DLR of 0.01 nM – 0.06 nM.

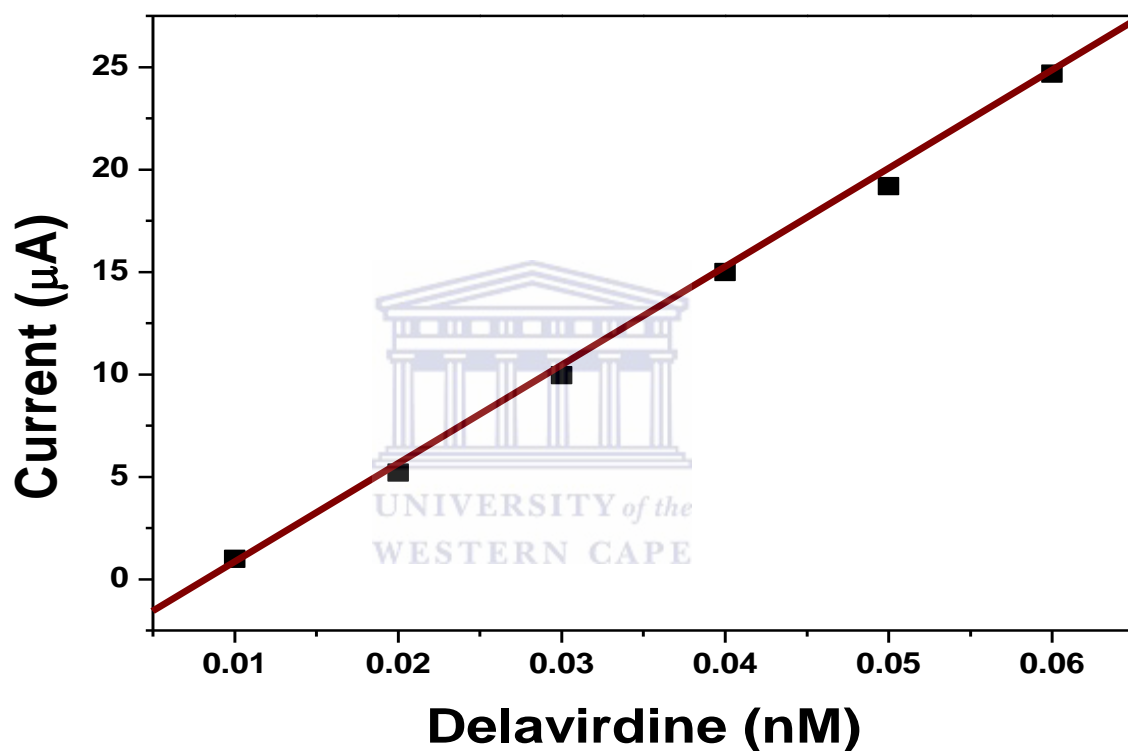


Figure 26: calibration curve from the linear range of hyperbolic curve for the determination of LOD.

Table 3: Detection limits for delavirdine by different detection methods.

Detection technique	LOD	Reference
A biosensor comprising enzyme CYP 3A4 immobilized onto (Cu(G2PPI)-co-PPy) star copolymer	0.025 nM	This study
Delavirdine detection using HPLC	17 μ M	Voorman, 2000
Surface plasmon resonance biosensor	190 nM	Elinder, 2010
Isocratic reversed phase high-performance liquid chromatography with fluorescence detection	1 nM	Veldkamp, 1999

Table 3 comprises of different detection techniques that can be used in the determination of delavirdine, the nanobiosensor devised in this study is the most practical device that can be used as it has the lowest detection limits than the other 3 techniques. This means that the (Cu(G2PPI)-co-PPy) star co-polymer-based nanobiosensor has the ability to detect concentrations as low as 0.025 nM which is a significantly low concentration that other techniques cannot detect.

Chapter 6

Conclusion and recommendations



UNIVERSITY *of the*
WESTERN CAPE

6.0 Summary

This chapter revisits the specific objectives of the study to report whether the aims of this dissertation were achieved, and to give an overview of the success and shortcomings of the study.

This study reports the successful development of a nanobiosensor which employed heme enzyme CYP3A4 for the detection of delavirdine a non nucleoside reverse transcriptase inhibitor anti HIV drug. The main objective of the study was to synthesize a copper poly (propylene imine)-co-poly pyrrole star copolymer through the functionalization of poly (propylene imine) dendrimer with pyrrole and to incorporate copper metal onto the functionalized poly (propylene imine); and use this as the platform of the nanobiosensor. Dendrimers and conducting polymers alike are attractive in their applications in the research of electrochemical biosensors due to their remarkable physicochemical and biological properties. In this study dendrimers have been used due to their porous structure which was suitable for the successful encapsulation and entrapment of copper nanoparticles and the enzyme CYP3A4. The conducting polymers and dendrimers enabled the immobilisation of the biological material (CYP3A4 enzyme) by providing a suitable microenvironment for biomolecules while retaining their biological activity by acting as a 3dimensional matrix. It is encouraging to report that FTIR, HRSEM, HRTEM and EDS studies showed the successful incorporation of the copper metal into the dendrimer. The (Cu(G2PPI)-co-PPy) star co-polymer was formed by dropcoating copper poly propylene imine-2Pyrrole onto Pt working electrode followed by the electrochemical polymerization of pyrrole onto the electrode. Thorough the characterization of the star copolymer using FTIR, HRSEM, HRTEM, EDS and CV indicated a stable platform for the immobilization of the enzyme CYP 3A4. The prepared star-co-polymer was used to serve as a point of attachment for the enzyme and act as a sufficient electron transfer mediator between the electrode surface and the redox enzyme centre of CYP 3A4. The results obtained from CV confirmed that the nanobiosensors was successful in the reductive catalysis of the delavirdine drug into respective water soluble and easy excretable metabolites. This is characterised by an observable increase in current for the analyte delavirdine. When the platform material was applied in the construction of the nanobiosensor, there was evidence of an increase in the current produced thus signifying excellent conductivity of the material ensuring good electron transfer within the system. This study is the first study to take advantage of the remarkable properties that are brought about by the combination of two polymer properties combined with a metal centre that has the

ability to act as a catalyst and source of electrons which are essential in the reduction process of delavirdine. Through the use of different characterisation techniques it was determined that (Cu(G2PPI)-co-PPy) star co-polymer was the best selection in the development of the nanobiosensor signified by the following parameters; DLR, LOD and sensitivity of 0.01-0.06 nM, 0.025 nM and 0.379 $\mu\text{A/nM}$ respectively. The highest observed plasma concentration (C_{max}) value of delavirdine found in plasma is 0.025-0.099 nM. The nanobiosensor developed in this study falls within the C_{max} value of delavirine indicating that the developed nanobiosensor can be used successfully in human samples. These results are indicative of a good nanobiosensor that can detect very low drug concentrations amongst HIV/Aids patients and to assist in the determination of the metabolic profile of these patients and ensure that they are given a proper dosage based on their individual metabolic rates.

In comparison to other studies using other techniques to determine the concentration of delavirdine such as HPLC and Surface plasmon resonance biosensor the (Cu(G2PPI)-co-PPy) star co-polymer-based nanbiosensor has the ability to detect concentrations as low as 0.025 nM which is a significantly low concentration that other techniques cannot detect.

6.1 Future work and Recommendations

- Studies need to be thoroughly done of the starting polymer materials so that better comparison can be done with the co-polymer.
- Square wave voltammetry experiments need to be performed and coupled to cyclic voltammetry.
- XRD needs to be done in order to corroborate with the FTIR findings to indicate whether the lattice parameters might show a decrease due to Cu incorporation during heat treatment of the formed complexes to ascertain that no structural changes occurred after modification as stated.
- Stability of the constructed biosensors need to be investigated.
- The response time of the constructed biosensors need to be determined through the performance of steady state amperometry experiments.

Chapter 7



7. References

1. Ajayi, R. F., Sidwaba, U., Feleni, U., Douman, S. F., Tovide, O., Botha, S., Baker, P., Fuku, X. G., Hamid, S., Waryo, T. T., Vilakazi, S., Tshikhudo, R., Iwuoha, E. I. 2014. Chemically amplified cytochrome P450-2E1 drug metabolism nanobiosensor for rifampicin anti-tuberculosis drug. *Electrochimica Acta* 128: 149-155.
2. Arntz, Y., Seelig, J. D., Lang, H. P., Zhang, J., Hunziker, P., Ramseyer, J. P. 2003. Label-free protein assay based on a nanomechanical cantilever array. *Nanotechnology* 14:86–90.
3. Azamian, B. R., Davis, J.J., Coleman, K. S., Bagshaw, C., Green, M. L. H. 2002. *Journal of American Chemistry Society* 124:12664-12991.
4. Baeumner, A. J., Cohen, R. N., Miksic, V., Min, J. RNA. 2003. Biosensor for the rapid detection of viable *Escherichia coli* in drinking water. *Biosensors and Bioelectronics* 18: 405–413.
5. Baleg, A. A. A., Jahed, N. M., Arotiba, O. A., Mailu, S. N., Hendricks, N. R., Baker, P. G., Iwuoha, E. I. 2011. Synthesis and characterization of poly(propylene imine) dendrimer – Polypyrrole conducting star copolymer. *Journal of Electroanalytical Chemistry* 652: 18-25.
6. Bard, A.J., Fan F. F., Kwak, J., Lev, O. 1989. Scanning electrochemical microscopy: Introduction and principles. *Analytical Chemistry* 61: 132-138.
7. Barner-Kowollik, C., Davis, T. P., H. Stenzel, M. H. 2006, Synthesis of star polymers using RAFT polymerization: What is possible. *Journal of Chemistry* 59: 719–721.
8. Baselt, D. R., Lee, G. U., Colton, R. J. 1996. Biosensor based on force microscope technology. *Journal Vacuum Science and Technology B* 14:789–793.
9. Bauer G, Pittner F, Schalkhammer T. 1999. Metal nano-cluster biosensors. *Mikrochimica Acta* 131:107–114.

10. Bhakshi, A. K., Bhalla, G. 2004. Conducting polymers: materials of the twenty first century. *Journal of Scientific and Industrial Research* 64: 715-720.
11. Belluzo, M. S., Ribone, M. E., Lagier, M. C. 2008. Assembling Amperometric Biosensors for Clinical Diagnostics. *Sensors* 8: 1366-1367.
12. Bistolos, N., Wollenberger, U., Jung, C., Scheller, F. W. 2005. Cytochrome P450 biosensors—a review. *Biosensors and Bioelectronics* 20: 2409-24415.
13. Boozer, C., Yu, Q., Chen, S., Lee, C., Homola, J., Yee, S. S. 2003. Surface functionalization for self-referencing surface plasmon resonance (SPR) biosensors by multi-step self-assembly. *Sensors and Actuators* 90: 22 – 30.
14. Borin, M. T., Cox, S. R., Herman, B. D., Carel, B., Anderson, J. R. D., Freimuth, W. W. 1997. Effect of fluconazole on the steady-state pharmacokinetics of delavirdine in human immunodeficiency virus-positive patients. *Antimicrobial Agents and Chemotherapy* 41(9):1892.
15. Brezoi, D. V. 2010. Polypyrrole films prepared by chemical oxidation in aqueous FeCl_3 solution. *Journal of Science and Arts* 1: 53-58.
16. Cai, H., Xu, C., He, P., Fang, Y. 2001. Colloid Au-enhanced DNA immobilization for the electrochemical detection of sequence-specific DNA. *Journal of Electroanalytical Chemistry* 510:78– 85.
17. Carr, F. D., la Porte, C. J. L., Pirmohamed, M, Owen, A., Cortes, C. P. 2010. Haplotype structure of CYP2B6 and association with plasma efavirenz concentrations in a Chilean HIV cohort. *Antimicrobial Agents and Chemotherapy* 65: 1889–1893.
18. Chan, S., Fauchet, P. M., Li, Y., Rothberg, L.J., Miller, B. L. 2000. Porous microcavities for biosensing applications. *Physical Status Solidi* 182:541–546.

19. Cui Y., We, Q., Park, H., Lieber, C. M. 2001. Nanowire nanosensors for highly sensitive and selective detection of biological and chemical species. *Science* 293:1289– 1292.
20. Choi, J., Lim, I. H., Kim, H. H., Min, J., Lee, W.H. 2001. Optical peroxide biosensor using the electrically controlled-release technique. *Biosensors and Bioelectronics* 16:141–146.
21. Chemla, Y. R., Grossman, H. L., Poon, Y., McDermott, R., Stevens, R., Alpert, M.D. 2000 Ultrasensitive magnetic biosensors for homogeneous immunoassay. *Proceedings of the National Academy of Science U S A* 97:14268– 14272.
22. Crumbliss, A. L., Perine, S. C., Stonehuerner, J., Tubergen, K. R., Zhao, J., Henkens, R. W. 1992. Colloidal gold as a biocompatible immobilization matrix suitable for the fabrication of enzyme electrodes by electrodeposition. *Biotechnology and Bioengineering* 40:483-493.
23. Cornell, B.A., Braach-Maksvytis, V. L. B., King, L. G., Osman, P. D. J., Raguse, B., Wieczorek, L. 1997. A biosensor that uses ion-channel switches. *Nature* 3: 387-580.
24. Cornell BA, Krishna G, Osman PD, Pace RD, Wieczorek L. 2001. Tethered bilayer lipid membranes as a support for membrane-active peptides. *Biochemical Society Transactions* 29:613-700.
25. D'Agostino, G., Alberti, G., Biesuz, R., Pesavento, M. 2006. Potentiometric sensor for atrazine based on a molecular imprinted membrane. *Biosensors and Bioelectron* 22:152–154.
26. Diallo, M., Chridtie, C., S waminathan , P., Johnson, J., G oddardi, W. 2005. Dendrimer Enhanced Ultrafiltration. 1. Recovery of Cu(II) from Aqueous Solutions

Using PAMAM Dendrimers with Ethylene Diamine Core and Terminal NH₂ Groups. *Journal of Biochemistry* 5: 500-515.

27. Edwards, M.A., Martin, S., Whitworth, A.L., Macpherson, J.V., Unwin, P.R. 2006. Scanning electrochemical microscopy: principles and applications to biophysical systems. *Physical Measurements* 27: 63–108.
28. Ellis, W. S., Hayhurst, G. P., Lightfoot, T., Smith, G., Harlow, J., Rowland-Yeo, K., Larsson, C., Mahling, J., Lim, C. K., Wolf, R. C., Blackburn, M.G., Lennard, M. S., Tucker, G. 2000. Evidence that serine 304 is not a key ligand-binding residue in the active site of cytochrome P450 2D6. *Journal of Biochemistry* 345: 565-571.
29. From Infection to AIDS. Boehringer Ingelheim HIV/AIDS
30. Gupta, B., Arun Kumar Singh, A. K., Melvin, A. A., Prakash, R. 2014. Influence of monomer concentration on polycarbazoleepolyindole (PCzePIIn) copolymer properties: Application in Schottky diode. *Solid State Sciences* 35: 56-66.
31. Hasler, J.A., Estabrook, R., Michael Murray, M., Pikuleva, I., Waterman, M., Capdevila, J., Holla, V., Helvig, C., Falck, J.R., Farrell, G., Laurence S. K., Simon D. S., Boitier. E., Beaune, P. 1999. Human cytochromes P450. *Molecular Aspects of Medicine* 20: 1-137.
32. Ingelman-Sundberg, M., Sarah C. Sim Alvin Gomez, S.A., Rodriguez-Antona. C. 2007. Influence of cytochrome P450 polymorphisms on drug therapies: Pharmacogenetic, pharmacoepigenetic and clinical aspects. *Pharmacology & Therapeutics* 116: 496–526.
33. Kauffmann, J.M., Guilbault, G.G. 1991. Potentiometric enzyme electrodes. *Bioprocess and Technology* 15: 63–82.
34. Kitade, T., Kitamura, K., Konishi, T., Takegami, S., Okuno, T., Ishikawa, M., Wakabayashi, M., Nishikawa, K., Muramatsu, Y. 2004. Potentiometric immunosensor

using artificial antibody based on molecularly imprinted polymers. *Analytical Chemistry* 76: 6802–6807.

35. Kerman, K.; Kobayashi, M.; Tamiya, E. 2004. Recent trends in electrochemical DNA biosensor technology. *Measurements of Science and Technology* 15: 1–11
36. Kirchheiner, J., Seeringer, A. 2007. Clinical implications of pharmacogenetics of cytochrome P450 drug metabolizing enzymes. *Biophysica Acta* 1770: 489–494.
37. Klajnert, B., Bryszewska, M. 2001 Dendrimers: properties and applications. *Acta Biochemical Polonica* 48 (1): 199-208.
38. Liao, J.C., Mastali, M., Gau, V., Suchard, M. A., Moller, A. K., Bruckner, D. A., Babbitt, J. T., Li Y, Gornbein, J., Landaw, E. M., McCabe, E. R. B., Churchill, B. M. 2006. Use of electrochemical DNA biosensors for rapid molecular identification of uropathogens in clinical urine specimens. *Journal of Clinical Microbiology* 44:561–570.
39. Liepold, P., Wieder, H., Hillebrandt, H., Friebel, A., Hartwich, G. 2005. DNA-arrays with electrical detection: A label-free low cost technology for routine use in life sciences and diagnostics. *Bioelectrochemistry* 67: 143–150.
40. Mapolie, S. F., J.L. van Wyk, J. L. 2013. Synthesis and characterization of dendritic salicylaldehyde complexes of copper and cobalt and their use as catalyst precursors in the aerobic hydroxylation of phenol. *Inorganica Chimica Acta* 394: 649–655.
41. Marassi, R., Nobili, F. 2009. Structural and chemical properties: Scanning Electron Microscopy. *Elsevier* 3: 758-766.
42. Mascini, M., Palchetti, I., Marrazza, G. 2001. DNA electrochemical biosensors. *Fresenius Journal Analytical Chemistry* 369: 15-22.
43. Marzolini, C., Telenti, A., Buclin, T., J. Biollaz, J., Decosterd, L. A. 2000. Simultaneous determination of the HIV protease inhibitors indinavir, amprenavir,

saquinavir, ritonavir, nelfinavir and the non-nucleoside reverse transcriptase inhibitor efavirenz by high performance liquid chromatography after solid-phase extraction. *Journal of Chromatography* 740: 43–58.

44. Mugo, J. N., Mapolie, S. F., van Wyk, J. L. 2010. Cu(II) and Ni(II) complexes based on monofunctional and dendrimeric pyrrole-imine ligands: Applications in catalytic liquid phase hydroxylation of phenol. *Inorganica Chimica Acta* 363: 2643–2651
45. Newkome, G. R., Shreiner, C. D. 2008. Poly(amidoamine), polypropylenimine, and related dendrimers and dendrons possessing different 1/2 branching motifs: An overview of the divergent procedures *Journal of Polymers* 49: 1-10.
46. Nicholson, R. S. 1965. Theory and Application of Cyclic Voltammetry for Measurement of Electrode Reaction Kinetics. *Analytical chemistry* 37: 1351-1354.
47. Ottaviani, F. M., Bossmann, S., Turro, N. J., Tomalia, D. A. 1994. Characterization of starburst dendrimers by the EPR technique. 1. Copper complexes in water solution. *116: Journal of American chemical society* 661-671.
48. Pan, D., Zuo, X., Wan, Y., Wang, L., Zhang, J., Song, S., Fan, C. 2007. Electrochemical Interrogation of Interactions between Surface-Confined DNA and Methylene Blue. *Sensors* 7: 2671- 2680.
49. Park, J., Moon, H. C., Kim, J. K. 2013. Facile Synthesis for Well-Defined A2B Miktoarm Star Copolymer of Poly (3-hexylthiophene) and Poly(methyl methacrylate) by the Combination of Anionic Polymerization and Click Reaction. *Journal of Polymer Science* 51: 2225-2226.
50. Pohanka, M., Skládal, P. 2008. Electrochemical biosensors – principles and applications. *Journal of Applied Biomedicine* 6: 57-61.
51. Ramakrishnan, S. 1997. Conducting polymers—from a laboratory curiosity to the market place. *Resonance* 2: 48–58.

52. Ramamurthy, N., Kannan, S. 2009. SEM-EDS analysis of soil and plant (calotropis gigantean linn) collected from industrial village, Cuddalore DT, Tamil Nadu India. *Journal of Biophysics* 19: 219–226.
53. Rambaut, A., Posada, D., Crandall, K. A and Holmes, E. C. 2004. The causes and consequences of HIV evolution. *Reviews* 5: 52-54.
54. Rassie, C., Olowu, R. A., Waryo, T. T., Wilson, L., Williams, A., Baker, P., Iwuoha, E. I. 2011. Dendritic 7T- polythiophene electro-catalytic sensor system for the determination of polycyclic aromatic hydrocarbons. *International Journal of Electrochemical Science* 6: 1949-1967.
55. Recognising the Symptoms. Boehringer Ingelheim HIV/AIDS.
56. Roberts, W.S., Lonsdale, D.J., Griffiths, J., Higson, S.P.J. 2007. Advances in the application of scanning electrochemical microscopy to bioanalytical systems. *Biosensors and bioelectronics* 23: 301–318.
57. Sadki, S., Schottland, P., Brodie, N., Sabouraud, G. 2000. The mechanisms of pyrrole electropolymerization. *The Royal Society of Chemistry* 29: 283–293.
58. Silley, P., Forsythe, S. 1996. Impedance microbiology: a rapid change for microbiologists. *Journal of Applied Bacteriol* 80: 233–243.
59. Shumyantseva, V. V., Bulko, T. V., Archakov, A. I. 2005. Electrochemical reduction of cytochrome P450 as an approach to the construction of biosensors and bioreactors. *Journal of Inorganic Biochemistry* 99:1051–1063.
60. Sridhar, J., Liu, J., Foroozesh, M., Klein Stevens, C.M. 2012. Insights on Cytochrome P450 Enzymes and Inhibitors Obtained Through QSAR Studies. *Molecules* 1: 9283-930.

61. Stuart, B. 2004. Infrared Spectroscopy: Fundamentals and Applications. *Analytical Techniques in the Sciences* 4: 510-600.
62. Sun, P., Laforge, F. O., Mirkin, M.V. 2007. Scanning electrochemical microscopy in the 21st century. *Physical Chemistry and Chemical Physics* 9: 802–823.
63. Taylor, P. J., Tai, C., Franklin, M. E., Pillans, P. I. 2011. The current role of liquid chromatography-tandem mass spectrometry in therapeutic drug monitoring of immunosuppressant and antiretroviral drugs. *Clinical Biochemistry* 44: 14–20.
64. Tonejc, A. 1999. High resolution electron microscopy HRTEM: image processing analysis of defects and grain boundaries in nanocrystalline materials. *Acta Chimica Slova* 46: 435-461.
65. UNAIDS World AIDS Day Report 2011, UNAIDS/WHO.
66. Varshney, E., Saha, N., Tandon, M., Shrivastava, V., Ali, S. 2012. Prevalence of poor and rapid metabolizers of drugs metabolized by CYP2B6 in North Indian population residing in Indian national capital territory. *Springer scopus* 1: 1-10.
67. Vassilev, K., Kreider, J., Miller, P. M., Ford, W. T. 1999. Poly (propylene imine) dendrimer complexes of Cu(II), Zn(II), and Co(III) as catalysts of hydrolysis of bis-(*p*-nitrophenyl) phosphate. *Real and functional polymers* 41: 205–212.
68. Veldkamp, A. I., van Heeswijk, R. P.G., Hoetelmans R. M.W., Meenhorst P. L., Mulder, J. W., Lange, J. M.A., Beijnen H. J. 1999. Rapid quantification of Delavirdine, a novel non-nucleoside reverse transcriptase inhibitor, in human plasma using isocratic reversed phase high-performance liquid chromatography with fluorescence detection. *Journal of Chromatography* 727: 151–157.
69. Voorman, R. L., Maio, S. M., Hauer, M.J., Sanders, P. E., Payne, N. A., Ackland, M.J. 1999. Metabolism of delavirdine, a human immunodeficiency virus type-1

reverse transcriptase inhibitor by microsomal cytochrome p450 in humans, rats and other species: probable involvement of CYP2D6 and CYP3A. *Drug metabolism and Disposition* 26: 631-638.

70. Voorman, R. L., Stephen M. Maio, S. M., Payne, N. A., Zhao, Z., Kenneth, A., Koeplinger, K. A., Wang, X. Microsomal Metabolism of Delavirdine: Evidence for Mechanism-Based Inactivation of Human Cytochrome P450 3A1. *The journal of Pharmacology and Experimental Therapeutics* 287: 381-387.
71. Van Loo, M.E., Lengowski, P.E. 2002. Automated Workstations for Parallel Synthesis. *Organic Process Research & Development* 6: 833-840.
72. Veldkamp, A. I., van Heeswijk, R. P. G., Hoetelmans, R. M. W., Meenhorst, P. L., Mulder, J. W., Lange, J. M. A., Beijnen, J. H. 1999. Rapid quantification of delavirdine, a novel non-nucleoside reverse transcriptase inhibitor, in human plasma using isocratic reversed-phase high-performance liquid chromatography with fluorescence detection. *Journal of Chromatography* 727: 151-157.
73. Wang, J., Cai, X., Rivas, G., Shiraishi, H., Farias, P. A. M., Dontha, N. 1996. DNA electrochemical biosensor for the detection of short DNA sequences related to the human immunodeficiency virus. *Analytical Chemistry* 68: 2629-2634.
74. Xiao, Y., Mia, H., Tang, S., Wu, H. 2013. Modeling antiretroviral drug responses for HIV-1 infected patients using differential equation models. *Advanced Drug Delivery Reviews* 65: 940-953.
75. Yang, H., LOPINA, S. T. 2003. Penicillin V-conjugated PEG-PAMAM star polymers. *Journal of Biomaterial Science Polymer Edition* 14: 1043-1056.
76. Yoshinobu, T., Iwasaki, H., Ui, Y., Furuichi, K., Ermolenko, Y., Mourzina, Y., Wagner, T., Nather, N., Schoning, M. J. 2005. The light-addressable potentiometric sensor for multi-ion sensing and imaging *Methods* 37:94-102.

77. Yuqing, M., Jianquo, G., Jianrong, C. 2003. Ion sensitive field effect transducer-based biosensors. *Biotechnology Advances* 21:527–534.
78. Zanger, U. M., Hofmann, H.M. 2008. Polymorphic Cytochromes P450 *CYP2B6* and *CYP2D6*: Recent Advances on Single Nucleotide Polymorphisms Affecting Splicing. *Acta Chimica. Slovenica* 55: 38–44.
79. Zanger U. M., Schwab. M. 2013. Cytochrome P450 enzymes in drug metabolism: Regulation of gene expression, enzyme activities, and impact of genetic variation. *Pharmacology and Therapeutics* 138: 103–141.
80. Zhou, M., Heinze, J. 1999. Electropolymerization of pyrrole and electrochemical study of polypyrrole: 1. Evidence for structural diversity of polypyrrole. *Electrochimica Acta* 44: 1733-1748.
81. Zolezzi, S., Spodine, E., Decinti, A. 2002. Electrochemical studies of copper (II) complexes with Schiff-base Ligands. *Polyhedron* 21: 55–59.
82. Zhu, R., Macfie, S.M., Ding, Z. 2005. Cadmium-induced plant stress investigated by scanning electrochemical microscopy. *Journal of Experimental Botany* 56: 2831–2838.

